ELEMENTA
Science of the Anthropocene

Jaffe, DA, et al. 2018. Scientific assessment of background ozone over the U.S.: Implications for air quality management. *Elem Sci Anth*, 6: 56. DOI: https://doi.org/10.1525/elementa.309

REVIEW

Scientific assessment of background ozone over the U.S.: Implications for air quality management

Daniel A. Jaffe[*,†], Owen R. Cooper[‡,§], Arlene M. Fiore[‖], Barron H. Henderson[¶], Gail S. Tonnesen[**], Armistead G. Russell[††], Daven K. Henze[‡‡], Andrew O. Langford[§], Meiyun Lin[§§] and Tom Moore[‖‖]

Ozone (O_3) is a key air pollutant that is produced from precursor emissions and has adverse impacts on human health and ecosystems. In the U.S., the Clean Air Act (CAA) regulates O_3 levels to protect public health and welfare, but unraveling the origins of surface O_3 is complicated by the presence of contributions from multiple sources including background sources like stratospheric transport, wildfires, biogenic precursors, and international anthropogenic pollution, in addition to U.S. anthropogenic sources. In this report, we consider more than 100 published studies and assess current knowledge on the spatial and temporal distribution, trends, and sources of background O_3 over the continental U.S., and evaluate how it influences attainment of the air quality standards. We conclude that spring and summer seasonal mean U.S. background O_3 (USB O_3), or O_3 formed from natural sources plus anthropogenic sources in countries outside the U.S., is greatest at high elevation locations in the western U.S., with monthly mean maximum daily 8-hour average (MDA8) mole fractions approaching 50 parts per billion (ppb) and annual 4th highest MDA8s exceeding 60 ppb, at some locations. At lower elevation sites, e.g., along the West and East Coasts, seasonal mean MDA8 USB O_3 is in the range of 20–40 ppb, with generally smaller contributions on the highest O_3 days. The uncertainty in U.S. background O_3 is around ±10 ppb for seasonal mean values and higher for individual days. Noncontrollable O_3 sources, such as stratospheric intrusions or precursors from wildfires, can make significant contributions to O_3 on some days, but it is challenging to quantify accurately these contributions. We recommend enhanced routine observations, focused field studies, process-oriented modeling studies, and greater emphasis on the complex photochemistry in smoke plumes as key steps to reduce the uncertainty associated with background O_3 in the U.S.

Keywords: Ozone; Air quality; Modeling; Clean Air Act; Urban air quality

1. Introduction: Definitions and sources of background ozone

Ozone (O_3) is a key secondary air pollutant associated with a number of health issues including asthma and premature death (Bell et al., 2004; Lippmann, 1993; Silva et al., 2013; Landrigan et al., 2018). Silva et al. (2013) estimate that ambient O_3 causes between 229,000–720,000 annual premature deaths globally, with 12,300–52,200 in North America alone. Ozone also adversely impacts growing vegetation, including crops, with a global estimated crop loss of $11–18 billion for the year 2000 (Avnery et al., 2011). Ozone was accordingly designated as a criteria air pollutant by the U.S. Clean Air Act (CAA) in the 1970s. The CAA requires that the U.S. Environmental Protection Agency (EPA) establish primary (to protect public health) and secondary (to protect public welfare) National Ambient Air Quality Standards (NAAQS) for O_3.

In the troposphere, O_3 is produced by photochemical reactions of nitrogen oxides (NO_x) with carbon monoxide (CO), methane (CH_4), and volatile organic compounds

* University of Washington, School of Science, Technology, Engineering and Mathematics, Bothell, Washington, US

† Department of Atmospheric Science, University of Washington, Seattle, Washington, US

‡ Cooperative Institute for Research in Environmental Sciences, University of Colorado, Boulder, Colorado, US

§ NOAA Earth System Research Laboratory, Chemical Sciences Division, Boulder, Colorado, US

‖ Department of Earth and Environmental Sciences and Lamont-Doherty Earth Observatory of Columbia University, New York, US

¶ U.S. EPA, Research Triangle Park, North Carolina, US

** U.S. EPA, Region VIII, Denver, Colorado, US

†† Georgia Institute of Technology, School of Civil and Environmental Engineering, Atlanta, Georgia, US

‡‡ University of Colorado, Department of Mechanical Engineering, Boulder, Colorado, US

§§ NOAA Geophysical Fluid Dynamics Laboratory, Princeton, New Jersey, US

‖‖ Western States Air Resources (WESTAR) Council and Western Regional Air Partnership (WRAP), Fort Collins, Colorado, US

Corresponding author: Daniel A. Jaffe (djaffe@uw.edu)

(VOCs). These O_3 precursors are emitted by fossil fuel combustion, agriculture, biomass burning, oil and gas production, and a variety of other industrial processes. Anthropogenic emissions of NO_x and some VOCs have decreased in the U.S. over the past several decades, and peak O_3 levels have declined in most areas of the U.S. as a result (Cooper et al., 2012; Simon et al., 2015; Strode et al., 2015). At the same time, new evidence has demonstrated adverse health effects at lower O_3 levels (US EPA, 2013) and the EPA recently strengthened both the primary and secondary NAAQS (US EPA, 2015). A monitor meets the standard if the 3-year average of the annual 4th highest maximum daily 8-hour average O_3 mole fraction (MDA8), called the "ozone design value (ODV)", is less than or equal to 70 parts per billion (ppb). An additional metric, the "W126 exposure index", can be used to assess the cumulative seasonal exposure of vegetation to O_3.

Regulation of locally formed O_3 is complicated by the fact that O_3 also has significant background levels in the troposphere. Observations from remote sites along the west coast of North America show that seasonal mean O_3 ranges from 30 to 50 ppb, thus the "background" air that enters the U.S. with the prevailing westerly winds already contains a substantial fraction of the 70 ppb standard. Observations and/or modeling show that, on some days, O_3 at a site may be enhanced by noncontrollable O_3 sources (NCOS), such as recent stratosphere-to-troposphere transport (STT), long-range transport from non-domestic sources, lightning, or photochemical production from natural NO_x and VOC precursor emissions including wildfires initiated by natural or human causes (Jaffe et al., 2004, 2005; Parrish et al., 2010; Ambrose et al., 2011; Wigder et al., 2013a; Langford et al., 2009, 2012). While foreign sources of pollution are theoretically controllable, these are beyond the control of any local jurisdiction, so for this discussion we include these in the NCOS category. In addition, foreign pollution is often mixed in with other types of NCOS (e.g., Cooper et al. 2004b; Ambrose et al., 2011), making it difficult to quantify these sources. The CAA provides several mechanisms, including Section 319b (Exceptional Events Rule (US EPA, 2016a, b)) and Section 179B (international transport), that offer policy solutions to account for high O_3 due to these noncontrollable sources (US EPA, 2013). We note that the EPA uses the term "exceptional events (EEs)" to consider days when surface O_3 is elevated above the NAAQS by episodic natural sources such as stratospheric intrusions or wildfires that cannot be "reasonably controlled" (EEs can also include episodic emissions of anthropogenic precursors if these were not reasonably controllable and are unlikely to recur at a specific location). EE influenced data can be excluded from the design value calculation if they are identified by the state agency and supported by evidence, which is then evaluated and approved by the EPA. Thus, excluding high O_3 caused by exceptional events may allow an area to be designated in attainment of the NAAQS. For areas that would otherwise violate the NAAQS because of international transport, Section 179B provides relief from penalties for failing to attain the NAAQS, but days affected by international transport are included in the calculation of the design value. In this review we focus on NCOS, rather than EEs, to consider more broadly the contributions of both international transport and EEs. Individual NCOS events can increase local surface O_3 levels on timescales ranging from hours to days before dissipating to become part of the tropospheric background. They are potentially important throughout the U.S., but the impact appears to be greatest in the western states where wildfires tend to be larger (Jaffe et al., 2013), deep stratospheric intrusions are more frequent (Skerlak et al., 2014), and transport from Asia is more important (Verstraeten et al., 2015).

The frequency of NCOS events, and thus higher background O_3, in the western U.S. makes it essential that we understand the sources of that O_3, and this requires careful analysis using both observations and models. In this review, we use the term "U.S. background O_3 (USB O_3)" as O_3 formed from NCOS plus anthropogenic sources in countries outside the U.S. (Dolwick et al., 2015). While USB O_3 incorporates the influence from NCOS, in our discussion, we focus on NCOS that elevate O_3 on a short-term basis (e.g., daily), to values above the seasonal mean USB O_3. Although the global CH_4 burden reflects both domestic and international emissions, we include its contributions in USB O_3, similar to previous work (e.g., Fiore et al., 2014a). Essentially, USB O_3 encompasses the contributions from natural and foreign sources of O_3 that cannot be controlled by precursor emissions reductions solely within the U.S. Since USB O_3 varies daily and is a function of season, meteorology, and elevation, quantification of USB O_3 on days that exceed the NAAQS is more relevant to air quality management than seasonal mean estimates. We note that some studies use the term "North American background (NAB) O_3", which is similar to USB O_3, but is defined as O_3 formed from natural sources plus anthropogenic sources in countries outside the U.S., Canada, and Mexico.

A quantitative understanding of USB O_3 is essential for air quality management in general, and for state and local efforts to meet the NAAQS in particular. This is especially true given the recent lowering of the NAAQS O_3 levels and the associated increasing relative importance of USB O_3 as domestic precursor emissions decrease. Primary tools used by states and the EPA to manage air quality are the State Implementation Plans (SIPs; US EPA, 2015) or Federal Implementation Plans (FIPs). These documents are federally-enforceable plans developed by and/or for states that identify how the state will attain and/or maintain the air quality standards. A key component of each SIP is the maintenance of a network of regulatory O_3 monitors that use standardized sampling methodologies, quality assurance, and siting requirements established by the EPA, along with other federal, tribal, state and local agencies. Knowledge of the sources contributing to the ambient levels on the highest O_3 days is important because controlling the domestic contribution to O_3 production affects the estimates of both the health benefits and the economic costs and benefits associated with achieving the NAAQS (US EPA, 2014c). This knowledge is also important for SIP development because it helps states identify the most effective emission control strategies.

Quantification of USB O_3 requires a chemical transport model (CTM) since it cannot be measured directly (e.g., Fiore et al., 2002, 2003; Zhang et al., 2009), but these models must be informed and evaluated using observations. In addition to USB O_3, an alternative useful metric for evaluating modeled mole fractions is "baseline" O_3, which is the distribution of O_3 observations at a rural or remote site that has not been influenced by recent, local emissions (HTAP, 2010). We note that this definition differs from the one adopted by a National Research Council (NRC) report (NRC, 2010), which defined baseline as "the statistically defined lowest abundances of O_3 in the air flowing into a country." We find the HTAP (2010) definition to be a more useful metric, since the lowest mole fractions may be associated with a particular season or transport pathway and therefore not representative of all conditions. Measurements of baseline O_3 are expected to be greater than model-estimated USB O_3 since the former includes some O_3 produced many days earlier by U.S. emissions that have been recirculated regionally or globally. In the following discussion, it is important to keep in mind that baseline O_3 is not the same as USB (or NAB) O_3, but both can be characterized by a seasonal mean, MDA8, 3-year ODV, and other statistical metrics. Because states develop their SIPs by evaluating O_3 response to emissions controls on the highest modeled O_3 days, an especially useful metric is the estimate of USB and NCOS O_3 on those days.

Natural, international, and domestic sources all contribute to observed surface O_3. **Figure 1** demonstrates how these sources contribute to O_3 mole fractions that are used in air quality management decisions. Depending on the magnitude of the sources, such as stratospheric intrusions or wildfires, these sources could be identified as EEs. However, the magnitude of the events and the ability of current data and tools to characterize it will impact whether specific episodes qualify as EEs. Which NCOS can be removed from the analysis may impact air quality management including SIPs.

In this review, we focus mainly on work completed since 2011 and build on earlier studies (NRC, 2010; McDonald-Buller, 2011). We address a number of scientific questions:

1. What methods have been used to identify and quantify background O_3 and what are the strengths, weaknesses, and uncertainties of these methods?
2. What do observations and models tell us about the spatial and temporal pattern, variability, trends, and episodic peaks in baseline and background O_3 across the continental U.S.?
3. What do observations and models tell us about the sources of background O_3?
4. How does USB O_3 impact local air quality and how do uncertainties in USB O_3 propagate into uncertainties in source attribution?
5. What strategies can be used to quantify daily, seasonal, and interannual variations in NCOS and what are the strengths and weaknesses of each method?
6. What strategies are needed to improve our estimates of baseline O_3, USB O_3, and NCOS and what are our recommendations for future research in this area?

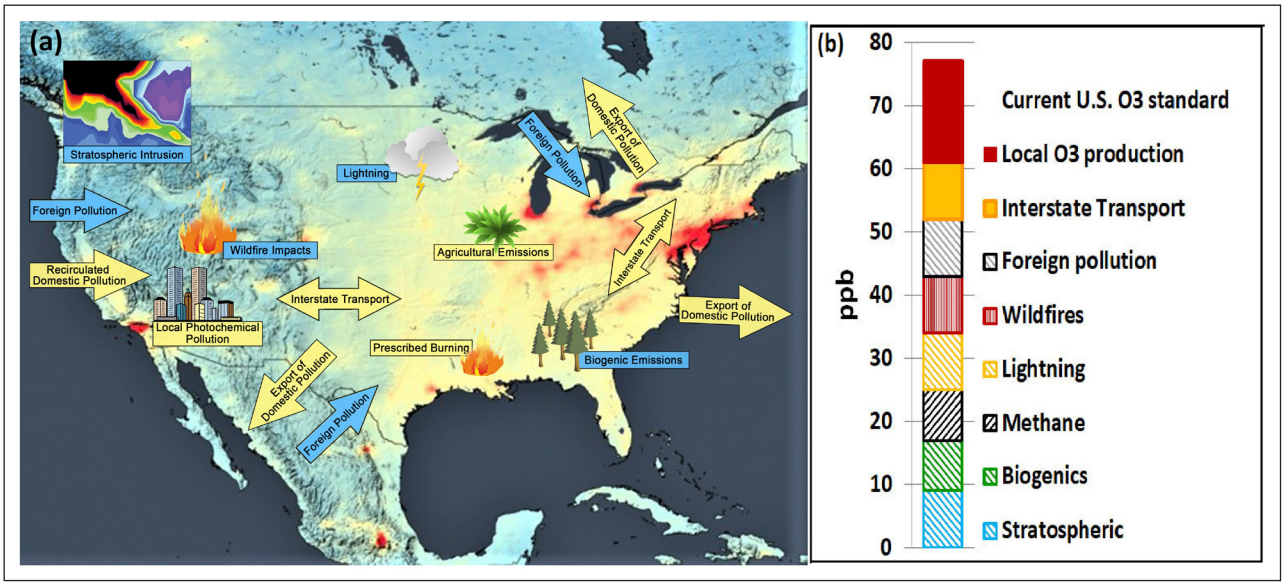

Figure 1: Conceptual models for O_3 sources (a) in the U.S. and (b) at a single location. (a) U.S. O_3 sources shown with yellow boxes or arrows represent domestic/controllable sources. Sources shown with blue boxes or arrows represent USBO/uncontrollable sources. Note that locations for each process are not specific to any one region. The base map shows satellite-observed tropospheric NO_2 columns for 2014 from the Ozone Monitoring Instrument (OMI) onboard the NASA Aura satellite (Credit: NASA Goddard's Scientific Visualization Studio/T. Schindler). NO_2 column amounts are relative with red colors showing highest values, followed by yellow then blue. We use the OMI NO_2 as a proxy to show local O_3 precursor emission sources. **(b)** The bar chart shows a theoretical example of how both domestic and USB O_3 sources combine to produce elevated O_3 at a specific location on any given day. Each source varies daily and there are also nonlinear interactions between USB O_3 sources and anthropogenic sources that can further add to O_3 formation, e.g., forest fires and urban emissions (e.g., Singh et al., 2012). DOI: https://doi.org/10.1525/elementa.309.f1

2. Spatial distribution of baseline O_3 in the U.S.

Most of the regulatory O_3 monitors in the continental U.S. are located in or near major population centers and not sufficiently isolated from upwind sources to provide representative information on the baseline O_3 inflow along the U.S. West Coast. One exception is the monitor maintained by the Washington Department of Ecology at Cheeka Peak [CP] on the coast of Washington State. NOAA (National Oceanic and Atmospheric Administration) also has a non-regulatory research monitor with a long-term data record about 850 km to the south of CP at Trinidad Head [THD] in northern California. Both of these monitors are located in the marine boundary layer, but the University of Washington operates another non-regulatory research monitor on a mountaintop site (Mt. Bachelor Observatory [MBO]) in central Oregon about 200 km from the coast. Twenty years of vertical profile data are also available from the NOAA ozonesonde program at Trinidad Head. **Figure 2** summarizes these observations for both spring and summer. What is clear from these data is that in the absence of local influences, both median baseline O_3 and the frequency of high O_3 events increase with altitude (Cooper et al., 2011; Musselman and Korfmacher, 2014). At low elevations, mean spring O_3 levels are about 10 ppb higher than summer values, whereas above 1 km, median spring and summer values are comparable, with summer showing a higher frequency of enhanced O_3 events. The small difference in median values for the THD sondes and MBO data at the same altitude has been attributed to large-scale dynamical patterns (Zhang and Jaffe, 2017). The positive vertical gradient and local orographic flows also cause the observations at MBO to show lower O_3 in the daytime, when air from the surrounding valley is lifted to the summit and higher O_3 at night, when the site is exposed to the free troposphere (Weiss-Penzias et al., 2006).

Altitude also has an influence on the ODV metrics as can also be seen by comparing nearby rural sites at different elevations. **Table 1** shows ODVs for pairs of rural monitoring sites in Oregon, Wyoming, and New Hampshire. In each case the higher elevation site (>1000 meters elevation difference) shows an ODV that is enhanced by at least 10 ppb compared to the lower elevation site. This reflects both the higher seasonal median O_3 and larger contributions from NCOS. For the Mt. Washington, New Hampshire site, and to a lesser extent the Centennial, Wyoming site, this could also reflect greater transport of domestic O_3, given that these sites are downwind of major U.S. source regions (e.g., Huang et al., 2013a). This is not the case for Mt. Bachelor, however, which receives minimal influence from U.S. anthropogenic sources (Ambrose et al., 2011). High O_3 levels at remote mountaintop sites such as Mt. Bachelor do not necessarily correspond to high values in

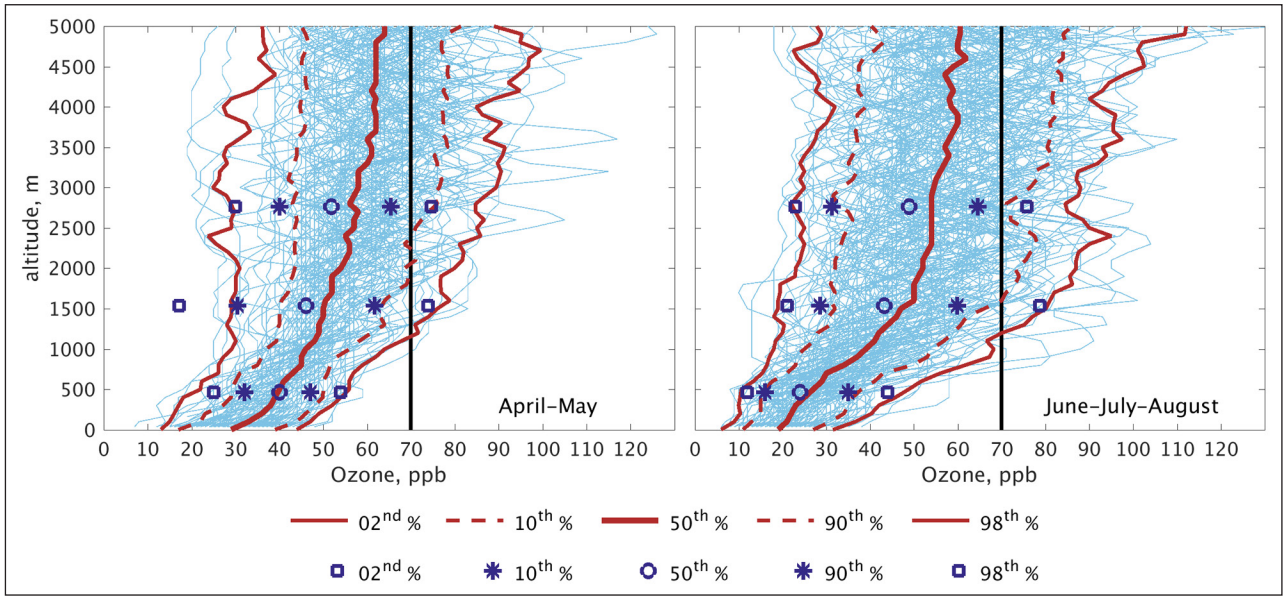

Figure 2: Vertical profiles of O_3 at Trinidad Head, Cheeka Peak, Mt. Bachelor Observatory, and Chews Ridge. Spring (left) and summer (right) vertical profiles (meters above sea level, m asl) as measured by ozonesondes (https://www.esrl.noaa.gov/gmd/) from Trinidad Head, California (2007–2017) and continuous surface observations at Cheeka Peak, Washington, at 500 m asl (2010–2016) (blue symbols), Mt. Bachelor Observatory, central Oregon, at 2763 m asl (2007–2016) (blue symbols), and Chews Ridge Observatory at 1500 m asl on the ridgeline of the Santa Lucia coastal mountain range in southern California (2012–2016) (blue symbols). For the Trinidad Head sonde data, blue lines represent individual sondes; red thin lines represent the 2nd and 98th percentiles, red dashed lines the 10th and 90th percentiles, and thick red lines the 50th percentile. From left to right, the blue symbols for the surface sites represent the 2nd, 10th, 50th, 90th and 98th percentiles of nighttime O_3 observations at Mt. Bachelor and Cheeka Peak and nighttime onshore O_3 observations at Chews Ridge. Black vertical lines reference the 70 ppb NAAQS. The data for Chews Ridge were provided by Ian Faloona (University of California Davis). The Cheeka Peak data were obtained from the EPA AQS network. The MBO data are from the University of Washington data archive (https://digital.lib.washington.edu/Researchworks). DOI: https://doi.org/10.1525/elementa.309.f2

Table 1: Comparison of O_3 ODVs for adjacent sites with differences in elevations >1000 meters (2013–2015).[a] DOI: https://doi.org/10.1525/elementa.309.t1

State	Site[b]	Coordinates	Meters asl	O_3 Design Value (ppb)[c]
Oregon	Bend	44.02°N, 121.26°W	1135	59
Oregon	Mt. Bachelor	43.98°N, 121.69°W	2763	77
Wyoming	Carbon	41.78°N, 107.12°W	2015	55
Wyoming	Centennial	41.36°N, 106.24°W	3178	66
New Hampshire	Camp Dodge	44.31°N, 71.22°W	451	57
New Hampshire	Mt. Washington	44.27°N, 71.30°W	1914	67

[a] Data are from the EPA AQS database (https://www.epa.gov/aqs) except for the non-regulatory Mt. Bachelor measurements, which are from the University of Washington data archive (https://digital.lib.washington.edu/Researchworks).
[b] In each state, the lower elevation site is in a small urban or rural location, whereas the elevated site is more remote.
[c] The MDA8s used in the ODV calculations use only data acquired with start hours between 0700 and 2300 local standard time. The ODV is the three-year average of the 4th highest annual MDA8, calculated after approved EE data have been excluded from AQS. For all sites listed here, no EE days were identified or excluded from the ODV calculation. Note that EEs have not been formally evaluated for the Mt. Bachelor data, since it is not a regulatory monitor.

more populated, lower elevation areas. Isolated high altitude sites have greater exposure to free tropospheric air that can be diluted as it is transported and mixed into the boundary layer (Wigder et al., 2013a). Furthermore, the O_3 lifetime is longer in the lower free troposphere than in near-surface air where it undergoes depositional loss to the surface and where chemical reaction rates may be enhanced in warmer, more humid air masses. The O_3 levels measured at mountain sites and nearby populated areas may be similar, however, if the boundary layers are sufficiently deep and well-mixed as is often the case in the Intermountain West (Langford et al., 2017).

3. Approaches used to quantify USB and NAB O_3

Most estimates of background O_3 have been made using regional CTMs such as the CMAQ (Community Multiscale Air Quality Modeling System) (Byun and Schere, 2006) and CAMx (Comprehensive Air Quality Model with Extensions) (Ramboll Environ, 2014) models that are initialized using lateral boundary conditions (BCs) derived from global models. In this section, we summarize the model approaches used to estimate USB O_3 and examine their different merits, limitations, and best uses. We note that different methods of employing CTMs may be best suited (scientifically or computationally) to a specific policy or research question. Biases owing to misspecification of emissions, errors in physical processes, choices regarding chemical mechanisms (Knote et al., 2015), model resolution (Lin et al., 2010), and plume dispersion (Rastigejev et al., 2010; Eastham and Jacob, 2017) may propagate into biases in the source attribution. In some cases, as described in more detail later, ad hoc methods for bias-correcting model estimated source attribution have been applied (e.g., Lin et al., 2012a, b; Lapina et al., 2014).

The most common modeling approach for quantifying USB O_3 is the "zero-out" method, whereby domestic anthropogenic emissions are set to zero (e.g., Zhang et al., 2014; Fiore et al., 2014a) to provide a direct estimate of the O_3 levels that would exist without domestic emissions. Nuances arise when applying the zero-out method to regional models wherein USB O_3 is transported into (and potentially out of) the regional modeling domain. For example, the regional boundary conditions used for defining USB O_3 may come from a global model run with U.S. anthropogenic emissions set to zero (e.g., Emery et al., 2012), or may be drawn from global model runs without any emissions perturbations (e.g., Lefohn et al., 2014). Huang et al. (2017) found that surface O_3 responses in a regional model over North America to changes in USB O_3 contribution from East Asia were smaller than those in the global models used to generate the boundary conditions. Zero-out scenarios also change O_3 production efficiency within the model domain causing the contributions from different sectors and regions to be non-linearly related. This is particularly obvious in the case of NO_x titration, which is removed when local emissions are zeroed, causing O_3 increases. This non-linearity can prevent the source contributions from adding up to 100% of the total modeled O_3 levels (Wu et al., 2009), which could be a concern when multiple model zero-out simulations from different source regions are combined.

Sensitivity methods can also be used to estimate USB O_3 and contributions by source. The most basic implementation of sensitivity modeling is direct perturbation modeling, where emissions from each source or region of interest (or contributions from the stratosphere) are reduced or increased by small amounts (e.g., ±20%; Wu et al., 2009; Galmarini et al., 2017) such that nonlinear O_3 responses are not typically triggered in polluted conditions (Cohan et al., 2005). At the extreme limit of perturbation methods (i.e., infinitesimally small perturbations), techniques such as adjoint modeling (Sandu et al., 2005; Zhang et al., 2009) and decoupled direct methods (DDM; Dunker et al., 1981; Hakami et al., 2004) efficiently calculate the local linear sensitivity of USB O_3 to numerous source contributions. These methods provide results suited for projecting changes in O_3 owing to small emissions perturbations (e.g., <20–50%; Reidmiller et al., 2009; Huang et al., 2017). Second-order correction terms can be applied to sensitivity approaches to estimate O_3

contributions caused by larger perturbations (Wu et al., 2009; Wild et al., 2012), or nonlinear changes can be evaluated using path-integral methods (Dunker et al., 2017). While these techniques can track sensitivities within a given model, they depend strongly on the emission inventories applied in that model. It is thus critical to evaluate uncertainties in historic and future source estimates, and how these uncertainties propagate into projections of specific O_3 metrics.

Tagging techniques track source contributions in models without perturbing emissions (Cohan and Napelenok, 2011; Grewe et al., 2010). Tagging relies on a set of rules for assigning each molecule of O_3 to a particular source. These sources may be defined as specific tropospheric production regions (e.g., Wang et al., 1998; Fiore et al., 2002) or the stratosphere (e.g., Lin et al., 2012a; Zhang et al., 2014). Other tagging approaches use chemical indicators of the factors limiting O_3 production (e.g., the ratio of hydrogen peroxide to nitric acid production, or the maximum incremental reactivity of VOC families) to assign O_3 to either NO_x or VOC sources, such as the CAMx OSAT (Ozone Source Apportionment Technology) and CMAQ ISAM (Integrated Source Apportionment Method) source tagging schemes (Ramboll Environ, 2014; Kwok et al., 2015). Tagging may also be defined through the addition of tracers to track the origin of precursor molecules such as NO_x (e.g., Emmons et al., 2012; Pfister et al., 2013) or VOCs (Butler et al., 2011). Other tagging rules include assignment preferentially to anthropogenic precursors (Ramboll Environ, 2014), or tagging of all O_3 precursors (NO_x, CO, and VOCs) such as in Grewe et al. (2010, 2017) and Guo et al. (2017), which leads to larger estimates of USB O_3 than sensitivity studies or tagging only one type of precursor. Ying and Krishnan (2010) developed a scheme that includes tracers for O_3 produced from individual species; the treatment of VOC impacts on radical species in this approach may underestimate contributions from reactive VOCs and overestimate those from less reactive VOCs (Kwok et al., 2015). Lefohn et al. (2014) define an Emissions-Influenced Background (EIB) that accounts for the decrease in the lifetime of USB O_3 caused by anthropogenic emissions. This diversity of tagging approaches can make direct comparisons across such studies challenging, and the differences in source attribution estimates as well as the computational cost of these methods make them less well suited than zero-out simulations for estimating USB O_3.

Several studies have compared USB O_3 estimates calculated using different methods. In one study, a tagging source apportionment method using CAMx was compared to a zero-out method using CMAQ. The two approaches were found to provide similar estimates of April–October mean NAB O_3 in rural areas, but in urban areas CAMx APCA (Anthropogenic Precursor Culpability Assessment) provided lower estimates of background O_3 compared to CMAQ zero-out (Dolwick et al., 2015). Other comparisons note that tagging is more appropriate for source attribution than for estimating responses to emissions changes (e.g., Collet et al., 2014). In cases strongly affected by nonlinearities of O_3 formation, the choice of source estimation method can lead to considerable differences (Grewe et al., 2010; Stock et al., 2013; Lapina et al., 2014; Emmons et al., 2012).

Parrish et al. (2017a) noted that the running average ODVs for sites in Southern California over the past 4 decades can be fit to a simple exponential decay function. They postulated that the asymptotic value of this fit is the same as USB O_3. However, it is difficult to compare this approach with modeling studies that use a more rigorous definition for USB O_3. To derive USB O_3 from the Parrish et al. (2017a) method, it is necessary to assume that U.S. emissions are asymptotically approaching zero, that emissions and ODVs are directly related, and that USB O_3 on ODV days is constant over the analysis time period. Because of these limitations, the "background ODVs" calculated in this manner are probably more representative of current baseline O_3, plus some unquantified contribution from U.S. anthropogenic emissions.

4. Spatial and temporal distributions of USB O_3

Here we review published work on spatial and temporal distributions of USB O_3 from CTMs and summarize consistent and robust patterns. We also identify discrepancies between estimates of USB O_3 and, if possible, the causes for these discrepancies. While a clear, quantitative synthesis across the published literature (Tables S1 and S2) is confounded by inconsistencies in the metrics reported and the time periods and regions considered, some robust patterns are evident and several CTMs have been able to capture the major features in the daily and seasonal surface O_3 patterns (Fiore et al., 2009; Reidmiller et al., 2009; Schnell et al., 2015).

The McDonald-Buller et al. (2011) review relied heavily on background O_3 estimates from the global GEOS-Chem (GC) model available at that time (Zhang et al., 2011). Major methodological advances since McDonald-Buller et al. (2011) include seasonal mean USB and NAB O_3 estimates from additional global and regional models (Table S1) and studies quantifying the influence of NCOS on surface O_3 distributions (Table S2). A broad set of modeling studies robustly shows that seasonal mean USB and NAB O_3 are usually largest at western U.S. high-altitude sites (Table S1), as expected from the general increase in O_3 with altitude in the troposphere (e.g., Newchurch et al., 2003; Logan et al., 1999). This spatial pattern was emphasized in the earlier McDonald-Buller et al. (2011) review paper and was based on observations of baseline O_3 and published USB and NAB O_3 estimates from the GC model.

Individual studies report different O_3 metrics and vary in their definitions of peak O_3 season, ranging from two to seven months, mostly in spring and summer. Synthesizing across these studies, we find a range of 15–65 ppb (Table S1) for seasonal mean USB O_3 (MDA8) over the U.S. The higher end of this range occurs over high-altitude western U.S. sites in spring when Asian pollution and transport from the stratosphere make their largest contributions (20–35 ppb; Table S2) and when the O_3 lifetime is longer than in summer (see Table S1). In the eastern U.S. and along the California coast, seasonal mean NAB O_3 from the GC model is in the range of 20–40 ppb (Fiore et al., 2014a)

and USB O_3 is similar for the California coast from CMAQ (Dolwick et al., 2015). Other O_3 metrics, such as those relevant for vegetation exposure, like W126, a 3-month integral that heavily weights high O_3, differ in their sensitivity to USB O_3 (e.g., Lapina et al., 2014, 2016; Huang et al., 2013b). A 3-model average NAB O_3 contributed 64–78% of the May–July daytime O_3 over the Intermountain West during 2010, but only 9–27% of the W126, which more strongly weights the highest O_3 levels (Lapina et al., 2014).

NCOS (and USB O_3) also show significant interannual variability, complicating direct comparisons across studies from different years. The studies in Table S2 summarize individual seasonal mean NCOS estimates, which include up to 25 ppb transported from the stratosphere, up to 10 ppb produced from lightning NO_x, and up to a few ppb from wildfires. Estimates for seasonal mean Asian influence are generally below 5 ppb (Table S2). Anthropogenic CH_4 is included in the USB O_3 estimates in Table S1, and has been estimated to contribute ~5 ppb to U.S. surface O_3 (Fiore et al., 2008, 2009). Near the U.S. borders with Canada and Mexico, international pollution transport enhances USB O_3 relative to NAB O_3 (Wang et al., 2009; Guo et al., 2018). In the southwestern U.S., seasonal mean USB O_3 is higher than in other regions during both spring and summer, and NCOS play a more important role on high O_3 days (Fiore et al., 2014a; Langford et al., 2017), although stratospheric intrusions occasionally decrease surface O_3 in the heavily polluted Los Angeles Basin (Langford et al., 2012).

At some locations, the influence from individual NCOS (**Figure 1**) leads to day-to-day variability in observed O_3 and modeled USB O_3. For example, at high-altitude western U.S. sites, USB O_3 correlates with simulated total ground-level MDA8 O_3, implying that USB O_3 drives day-to-day variations in observed O_3 (Fiore et al., 2014a; see their Figure 8). Other models consistently find western USB O_3 increases with observed (total) O_3 (Lefohn et al., 2014; Huang et al., 2015), although Dolwick et al. (2015) note that the fractional USB O_3 contribution is typically less for the highest modeled values. Numerous studies have shown that NCOS can contribute up to 30 ppb to the observed MDA8 at regulatory monitors due to deep stratospheric intrusions, especially at high-altitude sites (e.g., Langford et al., 2009, 2015a; Lin et al., 2012a, 2015a; Knowland et al., 2017) or from wildfires (Jaffe et al., 2004; Singh et al., 2012; Dreessen et al., 2016; Gong et al., 2017). Cross-border transport from Mexico or Canada can also contribute to significant variations in daily MDA8 values (Wang et al., 2009). Modeled USB O_3 also show these daily variations due to NCOS, with modeled USB MDA8 O_3 sometimes exceeding 70 ppb (Lin et al., 2012a, b; Zhang et al., 2014). Models will not necessarily capture the O_3 maximum on the highest observed days, implying uncertainty in the simulated partitioning of total O_3 into USB O_3 and other sources (Fiore et al., 2014a). Furthermore, even if a model captures the observations perfectly, it does not necessarily follow that the simulated source attribution is correct.

Figure 3 illustrates that the 4th highest NAB MDA8 value at rural locations in the NOAA GFDL AM3 model is much lower than the observed 4th highest MDA8 over most densely populated U.S. regions, but that NAB O_3 contributes to some of the highest observed days in the Intermountain West, Pacific Northwest, and along the U.S.–Canada border. At some high elevation sites, the annual 4th highest NAB MDA8 from AM3, averaged over 2010–2014, exceeds 60 ppb although we note that AM3 simulations may be biased high by too much transport from the stratosphere (Lin et al., 2012b; Fiore et al., 2014a). Over the eastern U.S., where **Figure 3** shows 4th highest NAB MDA8 values below 60 ppb, both AM3 and GEOS-Chem indicate that the highest O_3 events are typically fueled by U.S. anthropogenic emissions with little correlation between USB O_3 and total simulated O_3 (with the possible exception of some sites along the Gulf Coast; Figure 8 of Fiore et al., 2014a).

A few of the studies in Table S1 compared seasonal mean and daily NAB O_3 estimates across 2–4 models and found discrepancies in the magnitude and variability, both spatial and temporal, of NAB O_3 estimates for the MDA8 (Fiore et al., 2014a), daytime mole fractions, and the W126 (Lapina et al., 2014) O_3 metrics. The AM3 model generally simulates significantly higher seasonal mean values in both spring and summer (up to 20 ppb higher), compared to other models. Fiore et al. (2014a) concluded that differences in model estimates of NAB O_3 resulted primarily from different model representations of stratosphere–troposphere exchange, wildfire, and lightning sources (and their subsequent chemistry) as well as isoprene oxidation chemistry in the models. HTAP (2010) and Huang et al. (2017) show that Asian and other intercontinental O_3 sources also vary by model. Orbe et al. (2017) show how different convection schemes can have large influences on transport, even when using the same meteorological fields. Dolwick et al. (2015) applied two regional models to compare the zero-out and source apportionment approaches and found similar seasonal mean MDA8 USB O_3 estimates (after correcting for biases as large as ±10 ppb versus observations in each of the regional models compared to observations). Discrepancies between these USB O_3 estimates occurred most strongly in urban areas where anthropogenic emissions can lower background O_3 levels due to NO_x titration (Dolwick et al., 2015). Consideration of odd oxygen in the tracers used for source apportionment would minimize such discrepancies. Odd oxygen here would be defined as including $O_3 + NO_x$ to account for conversion of O_3 to NO_2 (by NO titration).

Uncertainty in estimates of USB O_3 can be difficult to consolidate across studies into an overall uncertainty estimate owing to differences in region, season, source apportionment method, and O_3 metrics considered in different works. Nevertheless, insight into the range of uncertainties can be gained from several studies that have considered multiple models or approaches in an internally self-consistent manner. While model diversity does not strictly represent the total model uncertainty (which must also consider bias against observations), it is still a useful measure of confidence in USB O_3 estimates. For example, the daytime NAB O_3 in Lapina et al. (2014) from

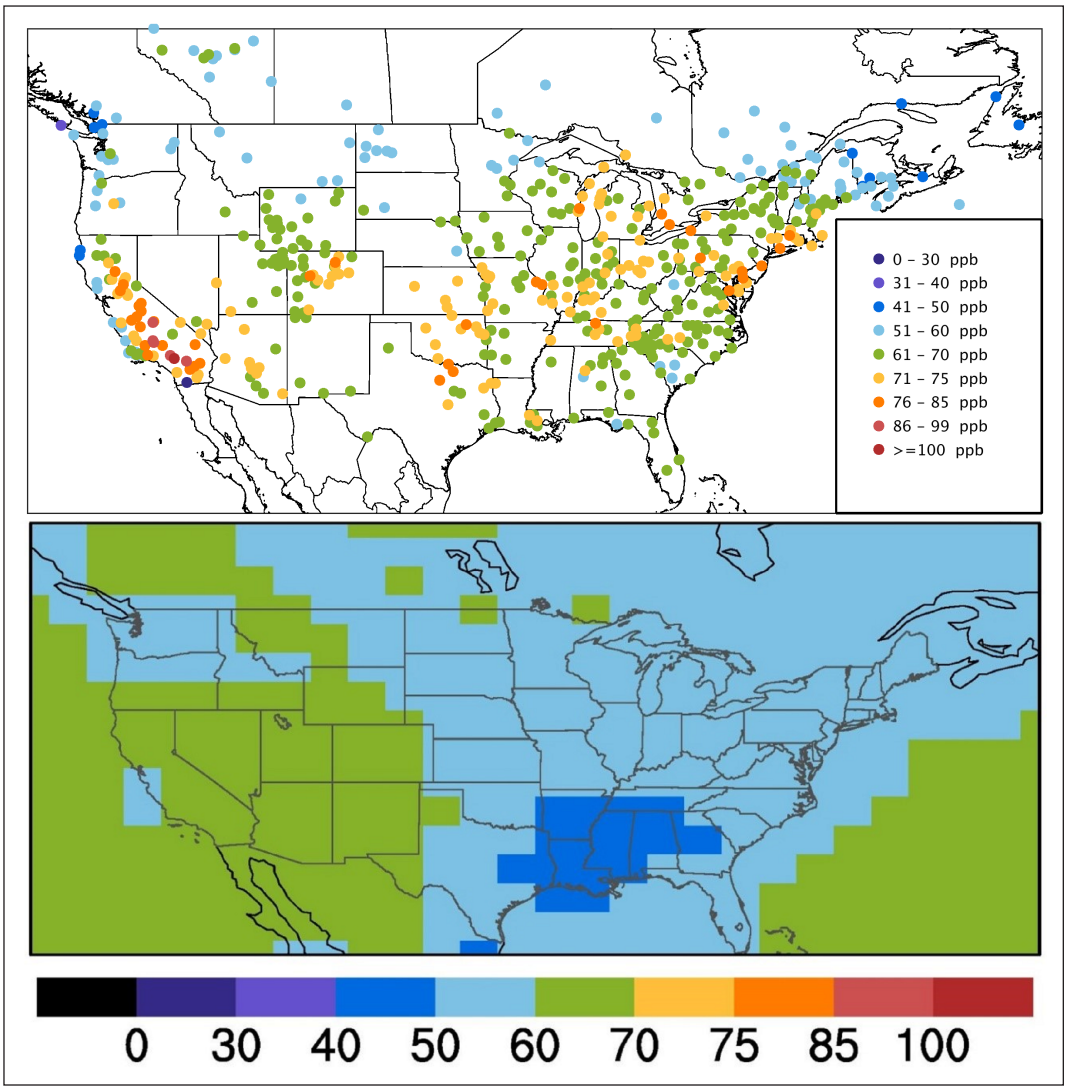

Figure 3: Annual 4th highest MDA8 O_3 observed and NAB modeled values. Annual 4th highest MDA8 O_3 value at all available rural O_3 monitoring sites in the U.S. and Canada, averaged over 2010–2014 (top). Annual 4th highest MDA8 NAB value averaged over 2010–2014, from a GFDL-AM3 model simulation with North American anthropogenic emissions zeroed out (bottom). Top figure provided by the Tropospheric Ozone Assessment Report (Schultz et al., 2017). Bottom figure from NAB O_3 simulation described in Lin et al., 2017. DOI: https://doi.org/10.1525/elementa.309.f3

three different global models showed modest differences over most regions of the U.S., but much more significant differences in NAB O_3 for the W126 vegetation index. In this case, the contribution from NAB O_3 to W126 can differ by a factor of 2 using different models. In Dolwick et al. (2015), two different regional models and source apportionment methods were used to estimate seasonal MDA8 USB O_3. They found that at over 75% of the locations, the differences were less than 2.5 ppb after the base models were bias corrected although we note that the same global model boundary conditions were used in each regional model. In Fiore et al. (2014a), estimates of MDA8 NAB from two global models differed by 1–10 ppb, depending upon region, season, and altitude. Hogrefe et al. (2018) evaluated surface O_3 simulations in a regional model using four sets of boundary conditions from different global models (AM3, MOZART, Hemispheric CMAQ, and GEOS-Chem). The largest differences exceed 10 ppb for seasonal mean O_3 observed at U.S. sites and reached 15 ppb on individual days. For two sets of boundary conditions, observation-model differences were much smaller (typically ±4 ppb). Qualitative synthesis by the authors of all these estimates of model differences and estimates of model biases suggests uncertainties in seasonal mean USB O_3 of about ±10 ppb.

Comparisons to observations are essential for assessing the fidelity of models used to quantify USB O_3 and NCOS and their spatial and temporal variability and lending confidence to their estimates. In some cases, different models bracket observed O_3 abundances (e.g., Fiore et al., 2014a), but in others, such as for ground-level O_3 over the southeastern U.S. in summer, systematic model biases exist (e.g., Travis et al., 2016). Travis et al. (2017) found that this pervasive positive summertime bias over the southeast U.S. is restricted to the surface and may reflect shortcomings in model resolution of asymmetric top-down and bottom-up vertical mixing. Systematic biases may also reflect missing (or poorly represented) loss processes (e.g., halogen

chemistry (Sherwen et al., 2017) or dry deposition (e.g., Val Martin et al., 2014)). Some of the studies in Table S1 have attempted to bias-correct USB or NAB O_3 estimates by simply assuming the bias is entirely due to USB O_3 (Lin et al., 2012b) or by assuming that the relative model contributions from individual sources are accurate such that USB O_3 is adjusted proportionally to its contribution to total simulated O_3 (Dolwick et al., 2015). The former approach assumes a single process causes the error whereas the latter assumes the model is missing a sink that acts on all O_3 regardless of the source (or overestimates O_3 from all sources equally). Models assimilating tropospheric satellite-based O_3 columns or aircraft-based profiles show improved model representation of western U.S. ozonesonde profiles (e.g., Huang et al., 2015) but would require assumptions to partition the adjustment into USB O_3 versus O_3 produced from U.S. anthropogenic emissions. While models adjusting emissions of O_3 precursors based on satellite data assimilation (e.g., Huang et al., 2015) could lead to improved estimates of USB O_3, this approach is still subject to errors in model transport and cannot differentiate between natural and anthropogenic sources occurring in the same model grid cell.

Although a single model may best represent a particular site or day of interest, a multi-model approach may best provide a general characterization of spatial, seasonal, and daily variability in USB O_3 until the root sources of individual model biases are clear. Future efforts would benefit from moving beyond abundance-based evaluations and towards process-based evaluation to demonstrate whether models capture the variability in observations attributable to USB O_3 and specific NCOS. This type of evaluation will require intensive field campaigns and long-term observations that measure not only O_3 but also related meteorological and chemical variables. Locations and times with inter-model differences with major implications for air quality management could guide targeted observations for evaluating process-level representation in the models. Efforts to coordinate multi-model approaches, as has been done for quantifying the influence of foreign anthropogenic emissions on surface O_3 under the Task Force on Hemispheric Transport of Air Pollution (HTAP, 2010; Galmarini et al., 2017), would facilitate a more systematic and rigorous assessment of our quantitative understanding of USB O_3 as represented across a suite of modeling systems.

Satellite observations enable new global model analyses (via data assimilation) and have made significant contributions to EE analyses (e.g., Fiore et al., 2014b). However, satellite data have not yet been able to retrieve O_3 mole fractions in the boundary layer and at the surface. Some satellite analyses have quantified tropospheric column O_3, either directly (e.g., Liu et al., 2010) or by difference (Ziemke et al., 2011). However, this situation is likely to change dramatically as several geostationary satellite instruments will be deployed in the next 5 years. This includes the U.S. Tropospheric Emissions: Monitoring Pollution instrument (TEMPO), the Korean Geostationary Environment Monitoring Spectrometer (Bak et al., 2013), and the European Sentinel-4 satellite (Zoogman et al., 2017). By measuring backscattered solar radiation in both the visible and near ultraviolet (290–740 nm) from a geostationary orbit, TEMPO should be able to distinguish boundary layer O_3 from that in the free troposphere and stratosphere, and provide hourly data for the continental U.S. on key O_3 precursors, such as nitrogen dioxide (NO_2) and formaldehyde (HCHO). Specifications for TEMPO call for a precision of 10 ppb for the 0–2 km and free tropospheric O_3 measurements. Thus, TEMPO should provide key constraints on modeled O_3 that can improve source and EE attribution (Zoogman et al., 2014, 2017). The satellite community has been engaged with regional air quality efforts via programs such as the NASA Air Quality Applied Sciences Team, and this has led to important partnerships between the scientific and regulatory communities (e.g., Fiore et al., 2014b; Witman et al., 2014).

5. Interannual variability and trends in baseline and USB O_3

Generalization of individual measurement and model results is complicated by the fact that background O_3 exhibits both long-term trends and substantial year-to-year variability. Observed year-to-year variations of surface O_3 show large-scale similarity across sites over the Intermountain West (Jaffe, 2011; Lin et al., 2017), indicating that the controlling processes operate across large scales. Both mean O_3 and the frequency of high O_3 events (>65 ppb) measured at western U.S. rural sites increased in the springs following the strong La Niña winters that occurred in 1998–1999, 2007–2008, and 2010–2011 (Lin et al., 2015a; Xu et al., 2017). Anomalously frequent high-O_3 events were also observed at Mt. Bachelor and urban sites downwind in April–May 2012. The enhanced O_3 in spring 2012 resulted in 3–6 days with an MDA8 greater than 70 ppb at several rural locations including Great Basin National Park and Lassen Volcanic National Park (Baylon et al., 2016). Using the AM3 model, Lin et al. (2015b) were able to capture the significant interannual variability and identify the cause. The highest MDA8 values at western U.S. rural sites occurred in the springs of 1999, 2011, and 2012, following La Niña patterns. The increased frequency of deep tropopause folds, linked to a cyclical amplification of the polar jet stream, is the key driver of year-to-year variability of springtime high USB O_3 events over the western U.S. (Lin et al., 2015b).

Large-scale variations in temperature, pressure, and airflow can also lead to substantial year-to-year variations in O_3 production, air mass stagnation, snowpack accumulation, and wildfire severity (Fiore et al., 2015; Mote et al., 2016; Gong et al., 2017; Jaffe and Zhang., 2017; Lin et al., 2017; Shen and Mickley, 2017). Interannual variability of surface O_3 in the Intermountain West during summer is found to correlate with wildfire severity (Jaffe, 2011; Jaffe et al., 2008). This correlation may also reflect common underlying correlations with temperature rather than a causal relationship between fire and O_3 (Zhang et al., 2014), as supported by a model with constant fire emissions, which captures the observed O_3 interannual variability (Lin et al., 2017). While wildfire emissions can enhance summertime monthly mean O_3 at individual sites by 2–8

ppb, high temperatures and the associated buildup of O_3 produced from regional anthropogenic emissions are also important to elevating observed summertime O_3 in the western U.S. (Jaffe and Zhang, 2017) and throughout the rest of the country (Lin et al., 2017).

Information on long-term baseline O_3 trends requires rural monitoring sites combined with methods that can select the data that are representative of air masses originating beyond the nation's borders. While boundary layer O_3 observations show more influence from local, continental, or marine sources, observations at high elevation sites (1.5–3.0 km asl) show greater influence from large-scale downward mixing of free tropospheric air, although they can also be influenced by transport of photochemically aged plumes from nearby urban areas or wildfires during summer (e.g., Ambrose et al., 2011). Studies of baseline O_3 trends have mainly focused on the limited number of well-positioned monitoring sites along the U.S. borders (Parrish et al., 2012, 2017b; Gratz et al., 2015; Zhang and Jaffe, 2017) and across the Intermountain West during spring due to the great interest in the potential impact of rising Asian emissions on U.S. surface O_3 (Jacob et al., 1999).

Cooper et al. (2012) found a tendency towards increasing O_3 at high elevation rural sites across the western U.S. in spring and no clear trend in summer over the period 1990–2010, despite stringent precursor emission controls in the U.S. that have decreased O_3 in urban areas (e.g., Russell et al., 2012). Extending the analysis to 1988–2014, Lin et al. (2017) found 0.2–0.5 ppb yr^{-1} increases in median springtime MDA8 O_3 measured at 50% of 16 western U.S. high elevation sites, with 25% of the sites showing increases across the entire O_3 mole fraction distribution. There is also evidence that O_3 increased in the mid-troposphere (500 hPa or ~5.7 km asl) above western North America during April–May at the rate of ~0.3 ppb yr^{-1} from 1995 to 2014 (Lin et al., 2015b).

Baseline O_3 trends on the West Coast of the U.S. have been determined at several of the surface and mountain sites described above, although the data records are relatively short. From 2004 to 2015, mean O_3 at Mt. Bachelor (2.8 km asl) has increased significantly: 0.62 ± 0.25 ppb yr^{-1} in spring, 0.66 ± 0.27 ppb yr^{-1} in summer, and 0.79 ± 0.34 ppb yr^{-1} in fall (Zhang and Jaffe, 2017). In the most recent analyses, marine boundary layer O_3 has remained unchanged at Cheeka Peak, Washington, and decreased at Trinidad Head in northern California (Parrish et al., 2017b). **Figure 4** shows these trends. The decrease of O_3 at Trinidad Head may be associated with a shift in transport pattern (as indicated by rapidly warming temperatures), while the spring increase at Mt. Bachelor has been attributed to changes in Asian emissions over the past decade and the summer increase attributed to regional wildfires (Zhang and Jaffe, 2017). The differences at these two sites, separated by a horizontal distance of 850 km, likely reflect the different influences of local processes, interannual meteorological variability, and changing USB O_3.

Attribution of baseline O_3 trends requires consideration of changes in global emissions, as well as regional climate variability, particularly in short data records. It is well established that O_3 formation depends on both temperature (e.g., Weaver et al., 2009) and humidity and changes in these climate variables must be considered when evaluating trends. For example, Bloomer et al. (2010) show that O_3 trends in the eastern U.S. between 1989 and 2007 were largely negative, despite temperature trends that were positive, indicating the dominant role played by emission reductions. Observed baseline O_3 trends have been compared with trends derived from a variety of global models: (1) CTMs driven with a single year's meteorology that repeats each year while emissions are allowed to change (Fusco and Logan, 2003; Reidmiller et al., 2009; Wild et

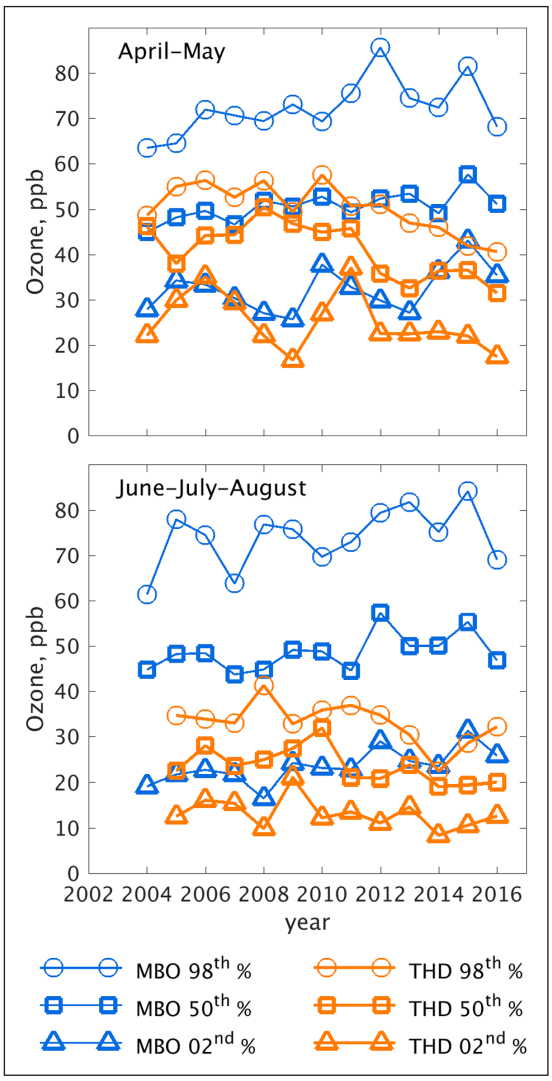

Figure 4: Interannual variability of baseline O_3 at Mt. Bachelor Observatory and Trinidad Head. Nighttime observations of baseline O_3 at Mt. Bachelor Observatory (blue) and baseline O_3 with daytime onshore wind conditions at Trinidad Head (orange) for the 2nd (triangles), 50th (squares), and 98th percentiles (circles). The range of values for the 98th percentile at Mt. Bachelor over the period 2004–2016 is 64–86 ppb during spring and 61–84 ppb during summer. The range of values for the 98th percentile at Trinidad Head over the period 2005–2016 is 41–58 ppb during spring and 22–41 ppb during summer. DOI: https://doi.org/10.1525/elementa.309.f4

al., 2012; Zhang et al., 2008), (2) free-running chemistry-climate models (CCMs) that generate their own weather, but are driven with historical emissions (Cooper et al., 2014; Lamarque et al., 2010; Parrish et al., 2014), and (3) multi-decadal hindcast simulations driven with observed meteorology and historical emissions (Brown-Steiner et al., 2015; Koumoutsaris and Bey, 2012; Lin et al., 2015b; Lin et al., 2014; Lin et al., 2017; Strode et al., 2015; Xing et al., 2015). The O_3 trends derived from observations are higher than those from CTMs with constant meteorology, and from free-running CCMs by a factor of two at some sites (e.g., Parrish et al., 2014). These discrepancies may partly reflect the influence of internal climate variability on observed O_3 (although we note that the reduced variability in CCMs may also reflect errors in their representation of chemistry and dispersion and from numerical diffusion, similar to CTMs whose meteorology is forced to match observed large-scale weather patterns). As the free-running CCM cannot reproduce the exact meteorological fields for the specific observational period, the model cannot be expected to capture the observed trend exactly (e.g., Lin et al., 2014, 2015a; Barnes et al., 2016). For example, Deser et al. (2012) have shown that summertime surface temperature projections for mid-century in some U.S. regions can vary from <1 up to 5°C for the exact same climate forcing scenario solely because of slight variations in the initial atmospheric state. As trends in O_3 are tied to meteorology, and it is unlikely if not impossible that a single climate model simulation would represent the internal variability exactly as manifest in the real atmosphere, CCMs cannot be evaluated in the same manner as CTMs driven by the observed meteorology. Furthermore, meteorologically-driven O_3 variability is large over western North America, leading to significant variations in O_3 trends between sites (Lin et al., 2015b).

One recent study using hindcast simulations forced with observed meteorology was able to match measured O_3 trends at rural western U.S. sites by narrowing the analysis to days when the airflow is predominantly from the North Pacific Ocean in the model (Lin et al., 2017). This study suggests that the common model-observation disagreement in baseline O_3 trends at western U.S. sites reflects an excessive offset from regional pollution decreases in the global models owing to their coarse resolution, which cannot fully resolve the observed baseline conditions. This shortcoming can be corrected by filtering model O_3 for baseline conditions using regionally emitted tracers in the model, such as CO (Lin et al., 2017).

A synthesis of available observations from the mid-1990s to the 2000s indicates increases in surface and free tropospheric O_3 across East Asia (see Supplementary Note 1 in the SI). Quantifying the effects of increasing Asian precursor emissions on O_3 in the U.S., relative to the effects of regional emission controls, has been an active research area in the last decade. Reidmiller et al. (2009) and Wild et al. (2012) used the HTAP simulations to show that regional emission controls over North America are 2–10 times as effective at reducing U.S. surface O_3 as the equivalent controls in Asia and Europe. Even so, Lin et al. (2017) demonstrated that the tripling of Asian NO_x emissions from 1990 to 2014 contributed 65% of modeled springtime background O_3 increases (0.3–0.5 ppb yr^{-1}) over the western U.S., outpacing O_3 decreases (<0.1 ppb yr^{-1}) attained via a 50% reduction of U.S. NO_x emissions. Increases in global methane contributed about 15% to the trend.

Detailed analyses of baseline O_3 trends along the U.S. southern and northern borders are limited in the peer-reviewed literature. Recent analysis by the Tropospheric Ozone Assessment Report (Schultz et al., 2017) of all available rural O_3 monitoring sites in the U.S. and Canada has provided some insight. While some O_3 data are available for urban sites in Mexico, there are no rural monitoring sites, greatly limiting our ability to understand Mexico's impact on U.S. baseline O_3. However, roughly 3 dozen rural sites are located across southern Canada with trends that are similar to those observed on the U.S. side of the border, based on the annual 4th highest MDA8 O_3 value. In general, there appears to be little change in O_3 across southern Canada in spring but there is an indication of decreasing O_3 in summer, presumably associated with Canadian NO_x emission decreases of 34% from 2000 to 2014 (Hoesly et al., 2018). The trend in O_3 transported from Mexico to the southern U.S. is not known from observations, but Mexican NO_x emissions have gone down by only 3% for 2000–2014 (Hoesly et al., 2018). Further details regarding observed O_3 trends across North America are provided in the SI (see Supplementary Note 2).

A number of studies have demonstrated that U.S. emissions and mole fractions of NO_x have declined substantially (Simon et al., 2015; Lamsal et al., 2015; Krotkov et al., 2016), but at the same time, there can still be substantial uncertainty in the absolute amounts (Hassler et al., 2016). One analysis suggests that the EPA National Emission Inventory (NEI) significantly over-estimates NO_x emissions from mobile and/or industrial sources (Travis et al., 2016). The most recent inventory shows that U.S. anthropogenic NO_x emissions decreased by 49% from 2000–2014 (Hoesly et al., 2018). It should be noted that fertilized agricultural and soil emissions of NO_x may be substantial, and may become more important as industrial emissions decline (Jaeglé et al., 2005; Almaraz et al., 2018). These emissions have higher uncertainties than the industrial emissions.

Peak O_3 levels and ODVs have decreased at most monitoring sites in the U.S., with the largest decreases in the eastern U.S. and in California (e.g., Simon et al., 2015). Figure S1 shows trends of the annual 4th highest MDA8 O_3 values (based on April–September observations) at all available rural O_3 monitoring sites in the U.S. and Canada, for the period 2000–2014. The great majority of sites show decreasing O_3 with p-values <0.10. **Figure 5** shows O_3 trends at high elevation (>1 km altitude) rural sites over the period 2000–2016. The analysis is applied to the 5th, 50th, and 95th percentiles of midday observations (1100–1600 local time) for spring (April–May) and summer (June–July–August) with the goal of assessing O_3 trends within air masses that are as regionally representative as possible. During spring only one site shows increasing O_3, Mt. Bachelor for the 50th and 95th percentiles (both trends in the range of 0.5–0.6 ppb yr^{-1}). In the case of Mt. Bachelor, only nighttime data are used here to focus on

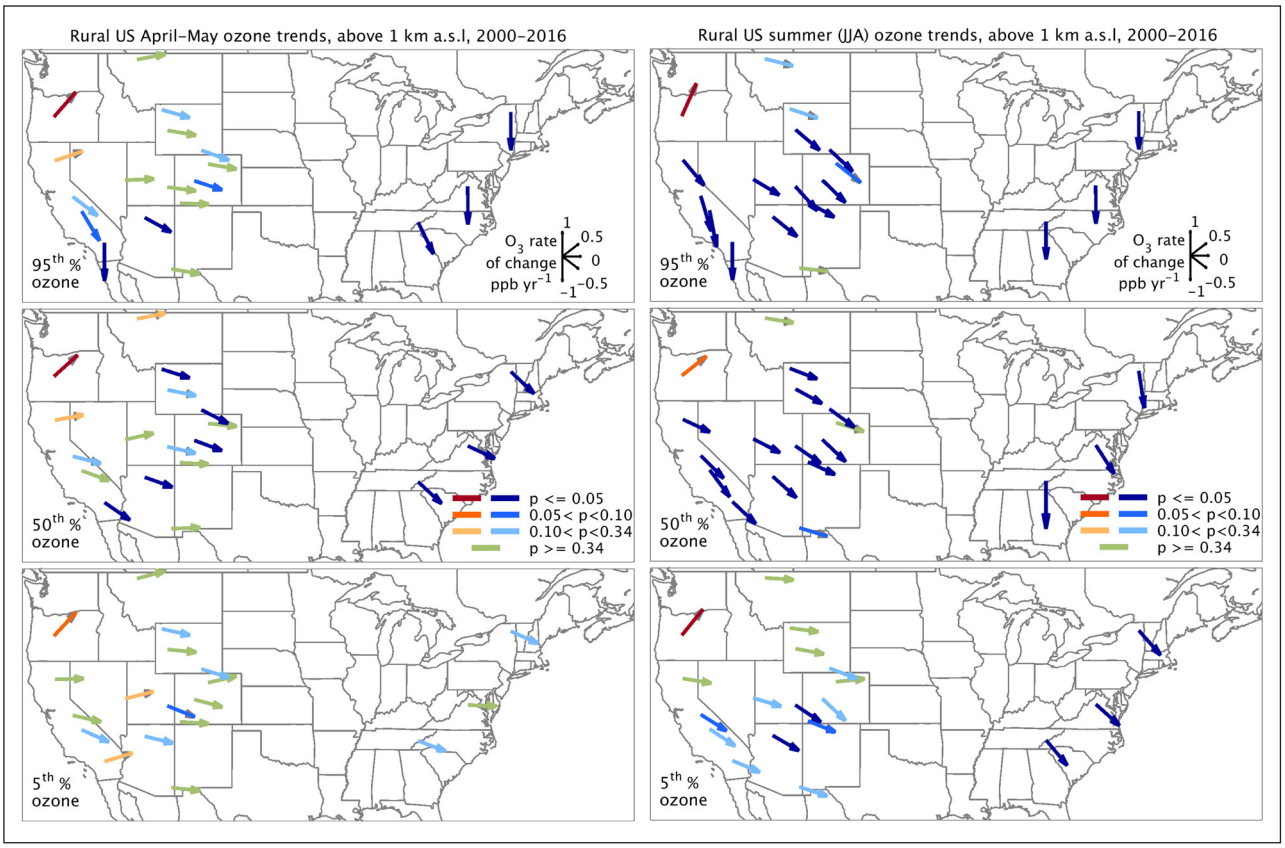

Figure 5: Mean O_3 trends for 2000–2016 at rural high elevation sites (>1 km asl). Spring trends (left) and summer trends (right). All sites used daytime data (1100–1600 local time.), except for Mt. Bachelor, where we use nighttime data to focus on baseline/free tropospheric air masses. Vector colors indicate the p-value associated with the linear trend at each site. DOI: https://doi.org/10.1525/elementa.309.f5

free tropospheric/baseline conditions, and the analysis at this particular site is limited to 2004–2016. Of the remaining western sites, most show no significant springtime trend while any significant trends are negative. In summer, Mt. Bachelor is again the only site with a statistically significant O_3 increase at the 50th and 95th percentiles (0.5 and 0.8 ppb yr^{-1}, respectively), likely due to recent increases in regional wildfire influence (Zhang and Jaffe, 2017). Otherwise, sites in the west and east show a clear tendency towards decreasing summertime O_3, especially in the upper tail of observations (95th percentile), presumably due to regional emissions controls. These results, limited to observations since 2000, differ from the conclusions of prior studies spanning the much longer periods of 1990–2010 (Cooper et al., 2012) and 1988–2014 (Lin et al., 2017), which showed a general increase of O_3 in spring and no consistent trend in summer. While most U.S. rural sites do not show significant springtime O_3 decreases since 2000, it appears that regional emission controls have led to widespread decreases in summertime O_3 at these sites, especially in the upper tail of observations.

Models may fail to simulate accurately the responses of O_3 to changes in U.S. emissions due to shortcomings in the underlying emission inventories. Several retrospective dynamic model evaluation studies using CMAQ tend to underestimate observed decreases in U.S. O_3 over the past decades (Foley et al., 2015; Xing et al., 2015; Zhou et al., 2013). Karamchandani et al. (2017) found that models more accurately simulate trends in observed O_3 in southern California when basin-wide VOC emissions were doubled. In contrast, for the eastern U.S., Travis et al. (2016) found that reducing industrial NO_x emissions, compared to the NEI, gave results that were more consistent with observations. Thus, emission inventory accuracy is key to model performance and inventories may have biases that vary by region. Inaccuracies in the magnitude of NO_x and VOC emissions introduce errors in the modeled sensitivity of O_3 to changes in precursor emissions. Wherever possible, O_3 sensitivities to precursor emissions should be evaluated directly as other sources of errors (e.g., inaccurate representation of changes in chemical or depositional loss rates) may also contribute to discrepancies between modeled and observed responses. To the extent that models misrepresent the contribution to O_3 from domestic sources, they will incorrectly estimate the relative fractions of controllable and background O_3.

We examined the change in the annual 4th highest MDA8 for 2000–2017 for 9 urban locations in the U.S. (San Bernardino, Chicago, Atlanta, Boston, Albuquerque, Sacramento, Salt Lake City, Denver, and Reno). In each location, we chose a single monitoring site with one of the highest ODVs in that urban area (Figure S2). From this we find that San Bernardino, Atlanta, Boston, Albuquerque, and Sacramento all show statistically significant downward trends in the 4th highest MDA8, whereas Chicago, Salt Lake City, Denver, and Reno show no significant trend

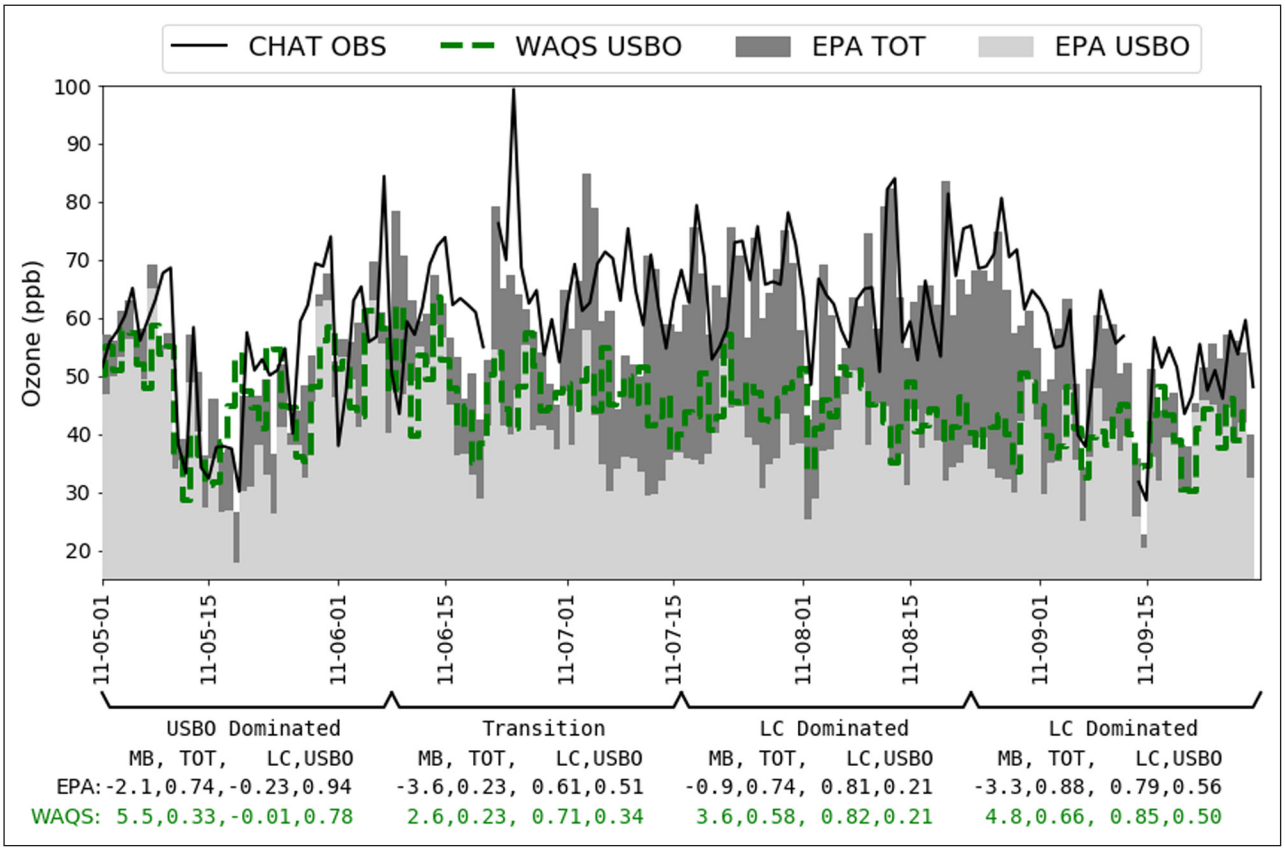

Figure 6: Observed and modeled MDA8 O_3 with USB O_3 from EPA model and WAQS for Chatfield. Observed O_3 (black lines), EPA model MDA8 O_3 (top of dark grey), EPA model USB O_3 (top of light grey), and WAQS USB O_3 (dashed green lines). For four simulation segments, the values below the axis give (for both models) the mean bias (MB), correlation (r) of total prediction with observations (TOT), correlation of local contribution (LC) with observations, and correlation of USB O_3 contribution with observations (USBO). DOI: https://doi.org/10.1525/elementa.309.f6

since 2000 (Table S3). Overall, the significant reductions in the urban areas are generally consistent with the rural O_3 trends shown in Figure S1. The negative trends in 4th highest MDA8 O_3 are linked to significant reductions in emissions of O_3 precursors, while at the same time there can be important regional differences in emission trends (e.g., emissions related to oil and gas extraction in some parts of the western U.S.) that can help explain some of the weaker trends. We note that three of the four locations with no significant trend are high elevation sites (Salt Lake City, Denver, and Reno). Trends in O_3 at these western sites might also be influenced by increasing wildfire activity. Exclusion of wildfire EEs would impact the trend in ODVs at these sites, if relevant states have submitted the EE documentation and EPA approves. Although we have examined only a single monitor in each urban area, this demonstrates the importance of accurate assessment of the USB O_3 contribution for these locations and regional modeling to quantify the controllable sources, as described in Section 6, below.

6. USB O_3 influence on regional air quality modeling: A western case study

Regulatory applications (e.g., SIPs) require models to represent accurately O_3 sources so that they can be used to examine emission scenarios and demonstrate future attainment of the NAAQS. This section shows one case study to highlight results as used in regulatory model applications. The regulatory treatment includes exclusion of identified exceptional days and focuses on the top 10 observed days. While this case study compares only two models, it provides insights into the relationships between regional model estimates of USB O_3 and observations. In particular, this analysis compares how simulated USB O_3 and other sources correlate and the implications for model performance as used in regulatory modeling.

The EPA Transport Assessment (US EPA, 2016c) and the Western Air Quality Study (WAQS, 2017) both independently simulated USB O_3 at 12-km resolution in Colorado for 2011. This is an ideal case study for USB O_3 relevant to state planning because the western states typically have high USB O_3 contributions, and because the Northern Colorado Front Range often experiences high O_3 levels that exceed the NAAQS. Both modeling systems use global simulations to provide time-varying boundary conditions (EPA: GEOS-Chem; WAQS: MOZARTv4) and quantified USB O_3 contribution as the sum of tagged boundary and natural sources of O_3 from May 1 to Sept. 29. Further details on both modeling systems are provided in the SI (see Supplementary Note 3). We compare simulations and contributions for two illustrative monitors: Chatfield (AQS 08-035-0004, hereafter CHAT), a regulatory relevant suburban monitor southwest of Denver, and Rocky Mountain

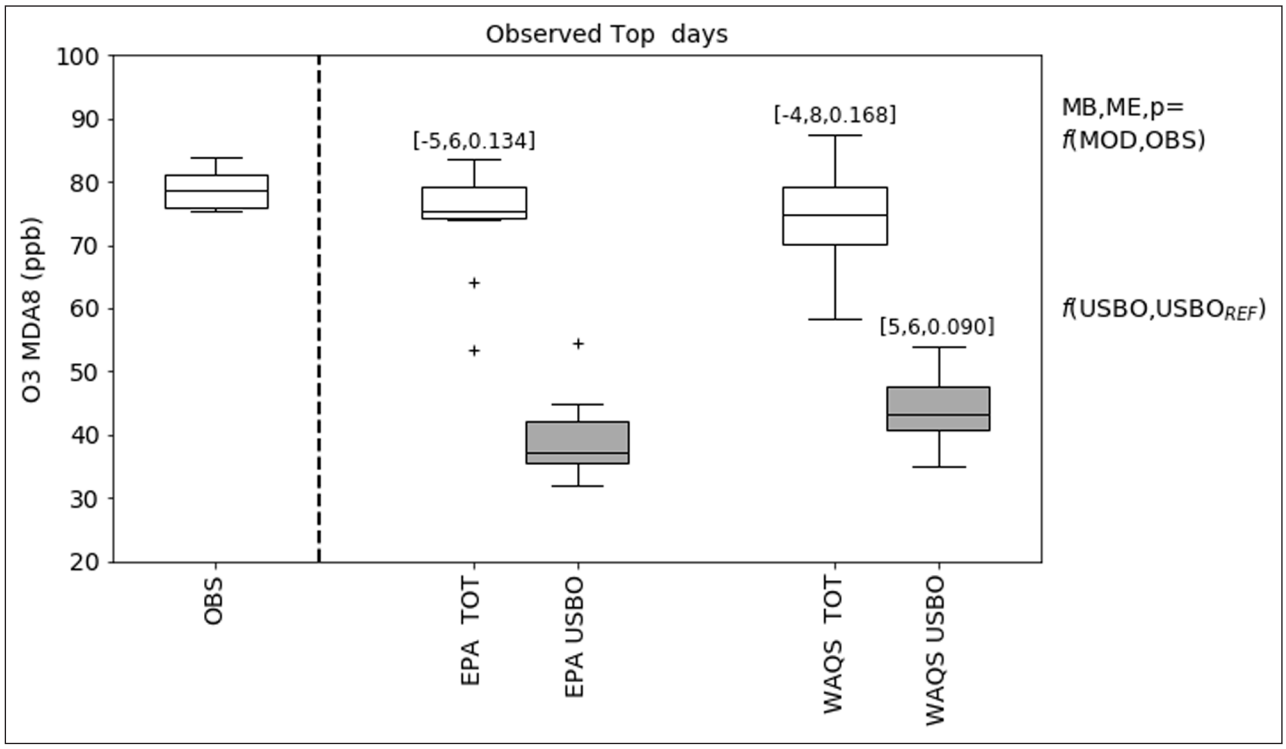

Figure 7: Observations, predictions, and USBO estimated by EPA and WAQS models for top 10 observed days. Observations (OBS), total predictions (TOT), and U.S. background O_3 (USBO) are shown. Mean bias (MB, ppb), mean error (ME, ppb), and the p-value for a t-test comparing model to observations are provided for TOT. Similar values are provided for WAQS USBO where EPA USBO is treated as the reference. Boxes denote the inter-quartile range (IQR), and whiskers extend to the min/max excluding outliers. Outliers are further than 1.5 times IQR below 25th percentile, or above the 75th percentile. (Two possible stratospheric intrusion days were removed.). DOI: https://doi.org/10.1525/elementa.309.f7

National Park (AQS 08-069-0007, hereafter RMNP), a relatively rural high elevation monitor to the northwest.

Figure 6 shows the observed and modeled MDA8 (EPA model only) and the USBO contribution (from both models) at CHAT. Figure S3 shows a similar comparison for RMNP. Monthly averaged biases at the CHAT monitor were marginally-negative in the EPA simulations (–2.5 ± 0.4 ppb) and marginally-positive in the WAQS simulations (4.0 ± 2.8 ppb), and both are consistent with literature synthesis of model performance (Simon et al., 2012). **Figure 6** suggests four distinct segments of performance and simulated contributions at CHAT that are related to NCOS contribution. The simulations start in a USB O_3 dominated regime (May 1 to June 7), go through a transition period (June 8 to July 15), and then end with two periods dominated by local contributions (July 16 to Aug 22 and Aug 23 to Sept. 29). During the USB O_3 dominated period, the EPA model had stronger correlation (r = 0.74) than the WAQS (r = 0.33), and WAQS had several days where USBO was greater than total observed O_3. During the transition period, both simulations performed poorly (r = 0.23). During the locally dominated periods, both simulations performed well. Table S4 shows additional correlations for individual model components. In general, there is a negative correlation between USBO and local contributions. Similar results were found at RMNP (see Figure S1), where the correlation was typically not as good as at CHAT. Based on this comparison, we find that periods associated with higher background contribution were associated with worse model performance. Thus, the simulations performed better during periods of sustained contribution (USB O_3 or local), simulations performed even better when USB O_3 and local contribution were not anti-correlated, and simulations performed best when local contributions were dominant.

Regulatory applications focus on high concentration days, so **Figure 7** examines the two models' performance on only the top 10 MDA8 O_3 days. The top 10 days were defined by the observed mole fractions. For this analysis, we excluded two days from the observations with suspected significant stratospheric influence (June 7th and 24th), consistent with guidance for regulatory modeling (US EPA, 2014a, and see further discussion in Supplementary Note 4 in SI). Both simulations have a negative mean bias (EPA: –5 ppb; WAQS: –4 ppb). The significance of the bias was evaluated using t-test. The null hypothesis is that the predicted and observed means are equal—put another way, that the predictions are on average unbiased. Despite large individual day biases on the top 10 days (range of +11 to –22 ppb), neither model bias was significant ($p > 0.05$).

We further compare USB O_3 between EPA and WAQS on the "observed top 10 days" to test if the choice of the modeling system produced significantly different contributions from NCOS and U.S. sources. Despite daily difference of up to 14 ppb, the average difference (5 ± 5 ppb)

was not significant ($p > 0.05$). The USB O_3 differences were comparable in magnitude to differences in local contribution (–4 ± 8 ppb) that were also not significant.

Our review of EPA and WAQS 2011 modeling for Chatfield highlights similarities between different models, but also confirms the need to improve modeling of background O_3. Correlations between observations and contributions at CHAT over the whole period are generally consistent with previous studies (US EPA, 2013; Zhang et al., 2011; Emery et al., 2012) showing that: (1) USBO is a significant fraction of total O_3 at the CHAT and RMNP sites; (2) the observed and predicted O_3 are most strongly correlated with the local contribution; and (3) boundary conditions are anti-correlated with the local contribution (see Table S4).

Both models perform well for average biases, but model correlation with observations is better when local contributions are dominant and when anti-correlation between local and USB O_3 contributions is weak. The boundary conditions derived from global models are dominated by USB O_3 in both models, which suggests a need for more research coupling global and regional models. The top 10 observed days are generally when the models perform best, and both models predict total O_3 that is consistent with the observations and each other. The finding that the models perform worst when USB O_3 and local contribution anti-correlation is strongest, or during transitions from USB O_3 to local contribution dominance, highlights the need for more research on USB O_3 and provides specific conditions for future studies.

7. Evidence for NCOS from observations and models

Individual NCOS events have long been associated with episodic increases in surface O_3, and much of our knowledge about their impacts in the U.S. and Canada has been inferred from routine ground-based measurements coupled with meteorological analyses (Ambrose et al., 2011; Fine et al., 2015; Jaffe and Zhang, 2017; Lefohn et al., 2012; Stauffer et al., 2017; Teakles et al., 2017; Wigder et al., 2013a, b) or with models and satellite retrievals (He et al., 2011; Lin et al., 2012a, b). These studies have been hampered by the sparsity of surface O_3 monitors in the western states where the impacts tend to be greatest (Gustin et al., 2015), and by limited free tropospheric measurements by aircraft (Yates et al., 2013), ozonesondes (He et al., 2011), or lidars (Kuang et al., 2012; Langford et al., 2018).

The episodic nature of some NCOS makes it difficult to target these sources with dedicated field studies, but opportunistic measurements have been made during field campaigns with other objectives (Langford et al., 2012; Ott et al., 2016; Sullivan et al., 2015). Long-range transport of O_3 and its photochemical precursors from Asia to the western U.S. was a focus of several recent campaigns including the California Research at the Nexus of Air Quality and Climate Change (CalNex) (Neuman et al., 2012; Ryerson et al., 2013) and Arctic Research of the Composition of the Troposphere from Aircraft and Satellites (ARC-TAS) (Huang et al., 2010; Jacob et al., 2010) missions. The impact of U.S. wildfires on O_3 in the West was also investigated during ARC-TAS (Singh et al., 2012) and other studies (Jaffe et al., 2008, 2013; Dreessen et al., 2016), and the influence of wildfires, long-range transport, and stratosphere-to-troposphere transport (STT) were foci of the Las Vegas Ozone Study (LVOS) (Langford et al., 2015a).

Most STT in the U.S. occurs through tropopause folds, tongues of upper troposphere/lower stratosphere (UT/LS) air extruded beneath the jet stream circulating around mid-latitude cyclones. These occur most frequently in winter when Rossby wave activity is at a maximum in the Northern Hemisphere, but the potential impact on surface O_3 is greater in late spring through early summer, when there is more O_3 in the lower stratosphere and deeper mixed layers can more easily entrain O_3 that reaches the lower troposphere (Langford et al., 2017). Descending stratospheric intrusions can also merge with biomass burning plumes (Brioude et al., 2007) or transported pollution (Cooper et al., 2004a, b; Lin et al., 2012b) and carry additional O_3 from these sources downward to the surface. Most tropopause folds are dissipated in the free troposphere and the transported O_3 becomes part of the free tropospheric background. Deep tropopause folds sometimes create localized spikes in surface O_3 (Langford et al., 2009), but they more frequently lead to smaller increases (<20 ppb) that can affect larger areas over several days (Lin et al., 2012a). They can also indirectly increase surface O_3 by fomenting the spread of wildfires due to their low humidity (Langford et al., 2015b). Several studies (e.g., Skerlak et al., 2014) have shown that the west coast of North America is one of the preferred regions for deep tropopause folds and there is growing evidence that the integrated contributions of frequent intrusions and co-mingled Asian pollution contribute to the springtime maximum in background O_3 in the southwestern U.S. and Intermountain West. STT events have also been implicated in exceedances of the O_3 NAAQS in the western U.S. (Langford et al., 2009; Langford et al., 2015a).

The contributions of STT to surface O_3 are not easily simulated using regional CTMs, which have traditionally included only the troposphere with no internal stratospheric processes. Regional simulations that use a global model to provide the lateral boundary conditions have shown qualitative success at simulating STT timing and location, but typically with significant under- (Emery et al., 2012; Zhang et al., 2014) or over-estimations (He et al., 2011). Under-estimations have often been attributed to poor horizontal resolution. Emery et al. (2012) showed several case studies where 12-km horizontal resolution was capable of reproducing transport to the surface. Inadequate vertical resolution and mixing is also a problem; for example, He et al. (2011) suggested that over-estimations of STT by the Environment Canada AURAMS CTM during the 2007 Border Air-Quality and Meteorology Study (BAQS-Met) were caused by the model having limited vertical resolution near the tropopause. For the under-estimations, Zhang et al. (2014) proposed a statistical correction to improve USB O_3 estimates. For the top boundary conditions in troposphere-only models, Xing et al. (2016) developed a seasonally and spatially varying potential vorticity (PV)-based function to characterize O_3

in the upper troposphere that improved springtime performance by the WRF-CMAQ model, but degraded it in fall. One outstanding challenge for model assessments of STT is how to treat O_3 that was originally produced in the troposphere, transported to the stratosphere, and then transported back to the troposphere, as part of a stratospheric intrusion. Zhang et al. (2014) show that different definitions for stratospheric O_3 can lead to a factor of 2 difference in the amount of O_3 identified as "stratospheric". While this does not change the total modeled O_3, it could lead to significant discrepancies in source contributions identified by different models.

Stratospheric intrusions can be identified in high-resolution reanalysis data (Knowland et al., 2017), and some global models have been successful in reproducing the surface contributions of STT. Simulations by GFDL-AM3 (Lin et al., 2012a, b), RAQMS (Pierce et al., 2003), and FLEXPART (Brioude et al., 2007) agreed well with lidar and in situ measurements made during the Las Vegas Ozone Study (LVOS) (Langford et al., 2017). He et al. (2011) also found good agreement between FLEXPART and surface and ozonesonde measurements made during several STT events in the BAQS-Met campaign. GFDL-AM3 estimated that deep STT can episodically increase surface O_3 by 20–40 ppb on days when observed MDA8 O_3 exceeds 70 ppb at western U.S. high elevation sites. GEOS-Chem can identify STT influence at the surface at high elevation sites but typically underestimates the contribution (Zhang et al., 2014).

Biomass burning can produce significant amounts of O_3, and wildfires are a growing concern (US GCRP, 2016). In the western U.S., forest management and climatic factors (e.g., drought and pine bark beetle infestations) have resulted in extensive tree mortality (Raffa et al., 2008), a significant increase in wildfire activity (Dennison et al., 2014), and deteriorating air quality in some areas (McClure and Jaffe, 2018). Agricultural burning is commonplace in the central and eastern U.S. (McCarty et al., 2007; Liu et al., 2016), but these fires are, in principle, controllable so are not considered NCOS. The chemistry in fire plumes is complex and highly variable, and does not always generate O_3. In a review of more than 100 studies on wildfire smoke, Jaffe and Wigder (2012) found that O_3 production generally increases for up to 5 days downwind, but with a very wide range in reported $\Delta CO/\Delta O_3$ enhancement ratios. While the majority of smoke plumes show some degree of O_3 enhancement, many studies have found no O_3 production or even O_3 loss. This reflects the large variability in NO_x and VOC emissions, plume heights, and downwind meteorology (Briggs et al., 2016; Baylon et al., 2015). Because wildfire emissions have high VOC/NO_x ratios (Akagi et al., 2011), O_3 production can increase when plumes pass over NO_x-rich urban areas (Singh et al., 2012; Gong et al., 2017).

Modeling O_3 production in wildfire plumes with Eulerian models is complicated by variable emissions, sub-grid processes, complex chemistry, uncertainties in emission magnitudes and injection heights, and the poorly characterized radiation fields in and around smoke plumes. Chemical transport models often over-predict the amount of O_3 produced near the fire (Jaffe et al., 2013; Zhang et al., 2014; Lu et al., 2016), although the simulated bias is strongly case dependent. For example, Baker et al. (2016) used CMAQ to model the O_3 produced from two wildfires that burned in 2011 and found frequent over-predictions of up to 60 ppb in hourly mole fractions. This may be mainly due to the presence of oxygenated VOCs in fire emissions, especially acetaldehyde (Akagi et al., 2011), which result in rapid sequestration of NO_x into PAN (Briggs et al., 2016; Müller et al., 2016). Herron-Thorpe et al. (2014) evaluated MDA8 O_3 at numerous sites in the Pacific Northwest for the summers of 2007 and 2008 and found that the AIRPACT-3 modeling system had a slight negative bias of 4.6 ppb with a mean error of 8.9 ppb over the two summers with significant fire emissions, but the authors also identified some large over-predictions for individual events. In summary, estimating wildfire O_3 production from Eulerian models is challenging, due to numerous factors, and these models need careful evaluation with observations.

Alvarado et al. (2015) developed a Lagrangian plume model to examine both O_3 and secondary aerosol formation from one prescribed fire in California. These results supported a critical role for rapid in-plume chemistry and NO_x sequestration (as PAN) to explain O_3 formation rates. A similar box model approach was successfully used by Müller et al. (2016). Both the Lagrangian and box model approaches avoid the problems of grid resolution, which is a major challenge for modeling fire plumes with 3D Eulerian models. Using a statistical model, combined with surface particulate matter (PM) and satellite data from the NOAA Hazard Mapping System, Gong et al. (2017) showed that wildfire impacts on MDA8 O_3 at 7 urban sites in the western U.S. range from negative values up to 33 ppb, including on days that had MDA8 values over 70 ppb. Plume models and statistical methods may provide useful estimates of O_3 production in fire plumes, but these approaches need further evaluation.

8. Methods to quantify the impact of NCOS on regulatory monitors as relevant to policy

The CAA recognizes that states and tribes should not be held responsible for sources of air pollution over which they have no control and provides several relief mechanisms to address NCOS. These include the Exceptional Events (EE) Rule (US EPA, 2016b) and CAA 179B provisions related to international transport (US EPA, 2016a). The effective implementation of these mechanisms depends on the ability to quantify the amount of O_3 from NCOS. Here we review several methods and assess the strengths and weaknesses of each approach.

The EPA has not yet published guidance on EE STT demonstrations; however, the EPA has approved EE demonstrations submitted by the state of Wyoming (WYDEQ, 2012; US EPA, 2014b) and other states (https://www.epa.gov/air-quality-analysis/treatment-air-quality-data-influenced-exceptional-events). These demonstrations can include measurements and model simulations showing layers of stratospheric air (characterized by elevated O_3, very low

humidity, and CO), increased potential vorticity (Xing et al., 2016), and transport into the boundary layer. These analyses provided qualitative demonstrations of substantial contribution from a stratospheric intrusion event but do not provide quantitative estimates of the contribution to O_3. While model simulations can provide quantitative estimates of stratospheric contributions, models sometimes fail to simulate accurately the observed surface O_3 during intrusion events and thus do not provide reliable quantitative estimates. Langford et al. (2015a, 2017) have shown that O_3 lidar measurements can be useful for directly observing layers of stratospheric air that descend deep into the troposphere and reach the surface boundary layer. Quantitative attribution of the stratospheric contribution can be improved if these observations are supplemented by surface measurements of O_3, CO, and $PM_{2.5}$ to help determine if the descending UT/LS air has mixed with international transport or wildfire plumes.

The EPA has published guidance on EE for wildfires (US EPA, 2016b) that describes three levels (or tiers) of technical analyses required to support an EE demonstration for a high O_3 day. All tiers include a narrative that demonstrates a clear causal relationship between the wildfire and an O_3 exceedance. When a fire is close to a site where monitored O_3 is typically low, Tier 1 uses trajectory analyses (e.g., HYSPLIT) and satellite imagery to show that the fire plume impacted the monitor. For Tier 2, fire emissions divided by distance from the monitor (Q/D) must be greater than 100/tons/day/km. Tier 2 additionally requires evidence that smoke from the fire impacted the monitor, such as monitoring data, satellite imagery, or photographs. For all other cases, a Tier 3 demonstration requires further additional evidence that supports the clear causal relationship between the wildfire and the O_3 exceedance. Typically, this includes an estimate of the wildfire contribution using matching day analyses, statistical regression models, or photochemical models, as described in more detail in US EPA (2016b). We note that the Q/D method, described in the EPA guidance, is based on previous methods for primary pollutants, and at present, there has been very little evaluation of the Q/D method with respect to O_3 produced from wildfires. A number of states have successfully demonstrated EEs for O_3 due to wildfire emissions, as described on the EPA website (https://www.epa.gov/air-quality-analysis/treatment-air-quality-data-influenced-exceptional-events).

Because of the difficulty of using Eulerian models to estimate wildfire O_3, EPA guidance also recommends use of a statistical approach. Statistical relationships have been developed to estimate O_3 as a function of a variety of meteorological indicators (e.g., Camalier et al., 2007). Depending on the location and meteorological data available, this method typically explains between 50 and 80% of the observed daily variability. Several studies have applied this method to estimate the O_3 contribution due to wildfires (CARB, 2011; Jaffe et al., 2013; Gong et al., 2017). In this approach, the statistical model is used to estimate the usual O_3 mole fraction for the observed meteorological conditions and the difference between the observation and the predicted, called the residual, is considered the additional O_3 due to some unusual source. While this approach cannot identify the cause for the additional O_3, it can give an indication of the magnitude of unusual contributions, if the residual is sufficiently large. Both the EPA guidance and Gong et al. (2017) discuss this method in more detail.

9. Conclusions and recommendations

The O_3 NAAQS has been strengthened several times since 1979 and most recently set at 70 ppb in 2015. With each downward step, the relative importance of background O_3 increases, as does the role of USB O_3 in air quality policy. Contributors to USB O_3, also called noncontrollable O_3 sources (NCOS), include natural precursor emissions (e.g., wildfires), long-range transport (e.g., from Asia, Canada, Mexico, or other countries), and stratospheric intrusions. When the standard is strengthened, daily variations in NCOS become more important and contribute to an increased frequency of MDA8 levels above the O_3 NAAQS. Model-calculated USB O_3 is greatest in March through June, with monthly mean MDA8 mole fractions at higher elevations in the west of up to 50 ppb and annual 4th highest MDA8 values exceeding 60 ppb at some locations. Lower elevation cities nationwide have monthly mean USB O_3 of 20–40 ppb during the O_3 season. Daily variations, particularly in spring and early summer, can be due to stratospheric intrusions mixed with Asian pollution, which can contribute to observed MDA8 values over 70 ppb. Elevated levels of O_3 or its precursors are also found in fire plumes, in some cases contributing to observed MDA8 O_3 values in excess of 70 ppb, particularly if fire plumes interact with NO_x-rich urban emissions.

While USB O_3 cannot be measured directly, baseline O_3 can, but suitably positioned observational stations are limited in number. Along the West Coast, baseline O_3 has increased since 2004 at the Mt. Bachelor Observatory in Oregon (2800 m asl) since 2004, while surface/marine boundary layer O_3 at Trinidad Head in northern California has decreased and O_3 at Cheeka Peak, Washington (500 m asl), is largely unchanged. However, we note that the marine boundary layer sites are less relevant to air quality beyond their immediate coastal surroundings. In contrast, the Mt. Bachelor site is more representative of the free tropospheric inflow to western North America, but the data record is relatively short. So, while there is a significant positive O_3 trend at this site, both meteorological variability and changes in USB O_3 are likely involved. In comparison, O_3 trends from most rural and urban sites in the U.S. show a consistent downward trend in the annual 4th highest MDA8 values since 2000, indicating the importance of regional emission reductions. The exceptions to this pattern are Chicago, Salt Lake City, Denver, and Reno, where trends in the annual 4th highest MDA8 at the most polluted monitors have not changed significantly since the year 2000.

Multiple methods have been used to estimate USB O_3, and, at times, significant differences can arise. These estimates of USB O_3 rarely include uncertainty. The lack of consistent reporting of model performance metrics hinders a quantitative uncertainty estimate. Uncertainty in

USB O_3 is estimated from many factors including differences between model results, model biases against observations, and interannual variations and trends. Baseline O_3 can vary significantly between years. At Trinidad Head in the marine boundary layer, spring (April–May) observed mean O_3 ranges from 32–48 ppb, based on data from 2004–2016. At Mt. Bachelor (2.8 km asl), the range in spring mean O_3 is 45–59 ppb over the same time period. For summer (June–August), the ranges are 18–29 ppb at the surface and 42–55 ppb at 2.8 km asl. Thus model simulations of USB O_3 must demonstrate the ability to capture these significant interannual variations with no significant bias. If systematic model biases are present, these must be explored so as to understand the underlying cause.

Given these limitations, our best estimate of the current uncertainty in the seasonal mean USB O_3 for typical years is ±10 ppb, which arises from model uncertainty, as discussed in Section 4. However, in some years, seasonal mean baseline O_3 is more than 5 ppb higher or lower than average (**Figure 4**) as a result of climate variability (e.g., El Niño), wildfire extent, and possibly other factors. Thus, for any given year, our predictive capability of USB O_3 could have an uncertainty greater than ±10 ppb, which arises from the modeling uncertainty compounded by the additional interannual variability. Uncertainty for shorter time periods can be higher (e.g., **Figure 6**) and accurate estimates of USB O_3 are especially important for MDA8 O_3 on days that exceed the NAAQS. In the case of potential EE determinations (e.g., due to fires or stratospheric intrusions), this level of uncertainty can have policy implications. In the case of SIP or NAAQS analyses, enhanced NCOS contributions that remain in the ODV (i.e., not excluded through the process defined in the Exceptional Events Rule) can directly impact the level of estimated controls required (US EPA, 2013). We note that some level of NCOS is always present as part of the mean USB O_3. Methods used to estimate USB O_3 and NCOS include both CTMs, as well as empirical approaches, and the difference between these methods is not well characterized. This is particularly true for wildfires that can occur at spatial scales smaller than those typically resolved by CTMs. In such cases, Lagrangian and statistical models can be used, but their application in such situations is still in its infancy.

The effort to quantify USB O_3 to date has lacked coordination and dedicated resources, as was noted in previous reports (NRC, 2010; McDonald-Buller, 2011; Cooper et al., 2015). With a lower O_3 NAAQS, local, state, and regional air quality planning organizations will increasingly need improved methods to quantify USB O_3 and NCOS with smaller uncertainties. To reduce these uncertainties, we have identified a series of research needs (in approximate order of importance):

1. ***An improved observation network is needed to better understand baseline O_3, USB O_3, and NCOS.*** While the U.S. has an extensive network of regulatory surface O_3 monitors, co-located measurements of key species (e.g., CO, NO_x, VOCs, $PM_{2.5}$, and speciated PM) that could be used to identify influences from stratospheric, foreign, natural, and/or biomass burning sources are made at only a few locations. In addition, most of the existing O_3 monitors are located near population centers because of regulatory requirements and limited funding, leaving much of the interior western U.S. under-sampled. A new generation of low-cost sensors could facilitate routine observations of O_3 and other key tracers at more surface monitoring sites (with careful validation), and an augmented baseline network with remote or high mountain locations and frequent vertical profiling (e.g., ozonesondes, lidar) (Langford et al., 2018) would improve identification of stratospheric, foreign, natural, and/or biomass burning sources. Key locations for enhanced observations are elevated locations and/or vertical profiles along the West Coast, in the Intermountain West, and along the U.S.-Mexico border.
2. ***Improved quantification of USB O_3 and the key processes controlling its distribution could be accelerated by one or more large-scale field experiments.*** Ideally, an experiment of this type would be conducted shortly after the TEMPO satellite instrument (Zoogman et al., 2014) becomes operational to provide large-scale, spatially and temporally continuous measurements across North America that can be directly linked to USB O_3 estimates. The experiments should also include a suite of baseline sites (expanded from the targeted network above), near-continuous vertical profiles of O_3 and precursor species, high mountain measurements, aircraft measurements, and multiple models operating over different seasons, including when USB O_3 is expected to be highest and during O_3 exceedances. Consideration should also be given to examining USB O_3 over multiple years to account for interannual variations. Past experience has shown that the success of large-scale field experiments requires a community-wide effort with observational and modelling assets drawn from multiple federal, state, and university institutions (e.g., CalNex and INTEX-B).
3. ***The ability of CTMs to quantify USB O_3 accurately and consistently across different temporal and spatial scales should continue to be improved to more effectively support policy and scientific applications.*** In general, CTMs have greatly improved our understanding of the sources of USB O_3. Continued progress will require process-oriented evaluations that include other key tracers wherever possible, with more attention paid to uncertainty and sensitivity analysis. Future modeling studies should report a consistent set of metrics including, at minimum, seasonal mean USB O_3, the USB O_3 on the observed annual 4th highest day and top 10 days (at the same time as the O_3 maximum), and distributions of USB O_3 binned by observed O_3 (e.g., at least for the ranges below 60 ppb, 60–70 ppb, and above 70 ppb), as well as standard model performance metrics identified in recent reviews (Simon et al., 2012). Model stud-

ies should also report evaluation metrics specific to the intended use (e.g., fire or stratospheric intrusion evaluations, if those results are reported). At their core, models rely on emission inventories. Particularly as larger industrial emissions are reduced, smaller source categories become more important. The role of deposition and chemical sinks in shaping O_3 distributions, including the USB O_3 component has received far less attention than the role of sources. We recommend that coordinated modeling efforts include diagnostics to allow exploration of inter-model differences in sinks as well as sources of USB O_3. In urban areas, USB O_3 estimates from models of different spatial resolutions may differ strongly across models due to NO_x titration. Additional work is needed to test whether consideration of odd oxygen (defined as O_3 + NO_x) reconciles such discrepancies. For hemispheric or global models that provide boundary conditions, it is necessary to archive four dimensional fields of all key tracers at 3-hour resolution at the regional model boundaries. Further, tracers or diagnostics are required that can distinguish between different types of NCOS at the boundaries. For detailed model inter-comparisons, full four-dimensional fields of O_3, VOC, CO, and NO_x, and key reaction products such as nitric acid, organic nitrates, total oxidized nitrogen species, and peroxides should be archived across the model domain. Comparison between models should focus on process-level analyses and model sensitivities, considering not only O_3, but also related species. Intercomparisons of model source apportionment estimates can be difficult to interpret because of differences in the approaches used to implement source attribution techniques. Instead, process-level intercomparisons should include sensitivity experiments, such as simulations with zero anthropogenic emissions, to assess differences in model estimates of natural and background O_3. Simulations with zero anthropogenic emissions will also provide improved estimates of background O_3 in urban areas where local NO_x emissions can titrate O_3. A better understanding of model uncertainty will require comparisons with baseline observations, targeted intensive campaigns, and coordinated model inter-comparisons.

4. ***Better methods for quantifying the impact of wildfires on O_3 (and PM) should be developed, tested, and compared.*** Wildfires can drive exceedances of both O_3 and PM, but the formation and dispersion associated with fires is poorly understood. Future progress will require more detailed observations such as those currently planned for several large-scale process-oriented studies (e.g., FIREX [https://esrl.noaa.gov/csd/projects/firex/whitepaper.pdf], FIRECHEM [https://espo.nasa.gov/FIREChem_White_Paper], and WECAN [https://www.eol.ucar.edu/field_projects/we-can]). The field experiments will require measurements upwind and downwind of wildfires to develop a detailed understanding of chemical processing, establish plume to plume variability, and improve smoke plume simulations by air quality models. Wildfire chemical processes simulated by Eulerian and Lagrangian models should be compared to statistical models to evaluate the efficacy of the three approaches.

Over the past decade, much progress has been made in our efforts to understand aspects of the USB O_3 problem (e.g., episodic stratospheric sources, interannual variability, wildfire contributions), but these efforts have lacked coordination. While our understanding of USB O_3 and the available tools have advanced, the uncertainties remain large and many of the conclusions and recommendations made here are similar to those made in the McDonald-Buller et al. review (2011). For a topic of such importance to air quality management and regional stakeholders, a more focused approach is needed. The strengthening of the O_3 standard and the increased importance of EE demonstrations heighten the need for the scientific, regulatory, and stakeholder communities to make substantial progress in improving the observations and tools to understand USB O_3.

Data Accessibility Statement

Mt. Bachelor Observatory data are available at the University of Washington data repository (https://digital.lib.washington.edu/researchworks/browse?type=subject&value=Mt.+Bachelor+Observatory). The Tropospheric Ozone Assessment Report Global surface O_3 datasets are available at https://doi.pangaea.de/10.1594/PANGAEA.876108.

Supplemental files

The supplemental files for this article can be found as follows:

- **Table S1.** Model estimates for background ozone (O_3) (multiple definitions).[a] DOI: https://doi.org/10.1525/elementa.309.s1
- **Table S2.** Model estimates for non-controllable ozone (O_3) sources (NCOS).[a] DOI: https://doi.org/10.1525/elementa.309.s1
- **Supplementary Note 1.** Observed ozone trends upwind of the western U.S. DOI: https://doi.org/10.1525/elementa.309.s1
- **Supplementary Note 2.** Observed ozone trends along the U.S. northern and southern borders. DOI: https://doi.org/10.1525/elementa.309.s1
- **Figure S1.** Trends in annual 4th highest MDA8 O_3 at rural sites in the U.S. and Canada. DOI: https://doi.org/10.1525/elementa.309.s1
- **Figure S2.** Annual 4th highest MDA8 O_3 for one site in each urban area. DOI: https://doi.org/10.1525/elementa.309.s1
- **Table S3.** Linear trends and t-test results comparing 2000–2017 4th highest annual MDA8 values in 9 representative urban areas.[a] DOI: https://doi.org/10.1525/elementa.309.s1
- **Supplementary Note 3.** EPA and WAQS modeling platforms. DOI: https://doi.org/10.1525/elementa.309.s1

- **Figure S3.** Observed and modeled MDA8 O_3 for Rocky Mountain National Park (RMNP) monitor. DOI: https://doi.org/10.1525/elementa.309.s1
- **Table S4.** Correlation matrix for O_3 observations (OBS), predictions (Mod), and contributions at Chatfield.[a] DOI: https://doi.org/10.1525/elementa.309.s1
- **Supplementary Note 4.** Rationale for excluding stratospheric intrusion days in analysis. DOI: https://doi.org/10.1525/elementa.309.s1

Acknowledgements
We thank Ian Faloona (University of California Davis) for providing the data for Chews Ridge (shown in Figure 2). We thank Martin G. Schultz et al. (2017, Tropospheric Ozone Assessment Report, links to Global surface O_3 datasets, *PANGAEA*, https://doi.pangaea.de/10.1594/PANGAEA.876108) for providing Figures S1 and S2.

Funding information
Support for a public workshop to discuss this review was provided by the American Petroleum Institute (API) and the Western States Air Resources Council. (The workshop agenda can be found at https://www.wrapair2.org/calendar/viewitem.jsp?&cal_item_id=13124.)

We acknowledge support for participation from the following grants: NASA HAQAST #NNX16AQ20G (AMF); NASA HAQAST #NNX16AQ26G (DKH); NSF #1447832 (DAJ); and NASA #NNX16AQ29G S02 (AGR).

Competing interests
The authors have no competing interests to declare.

Author contributions
All coauthors contributed to conception and design, contributed to acquisition of data, contributed to analysis and interpretation of data, drafted and revised the article, and approved the submitted version for publication.

References
Akagi, SK, Yokelson, RJ, Wiedinmyer, C, Alvarado, MJ, Reid, JS, Karl, T, Crounse, JD and **Wennberg, PO.** 2011. Emission factors for open and domestic biomass burning for use in atmospheric models. *Atmos Chem Phys* **11**: 4039–4072. DOI: https://doi.org/10.5194/acp-11-4039-2011

Almaraz, M, Bai, E, Wang, C, Trousdell, J, Conley, S, Faloona, I and **Houlton, BZ.** 2018. Agriculture is a major source of NO_x pollution in California. *Science Advances* **4**(1). DOI: https://doi.org/10.1126/sciadv.aao3477

Alvarado, MJ, Lonsdale, CR, Yokelson, RJ, Akagi, SK, Coe, H, Craven, JS, Fischer, EV, McMeeking, GR, Seinfeld, JH, Soni, T, Taylor, JW, Weise, DR and **Wold, CE.** 2015. Investigating the links between ozone and organic aerosol chemistry in a biomass burning plume from a prescribed fire in California chaparral. *Atmos Chem Phys* **15**(12): 6667–6688. DOI: https://doi.org/10.5194/acp-15-6667-2015

Ambrose, JL, Reidmiller, DR and **Jaffe, DA.** 2011. Causes of high O-3 in the lower free troposphere over the Pacific Northwest as observed at the Mt. Bachelor Observatory. *Atmos Environ* **45**(30): 5302–5315. DOI: https://doi.org/10.1016/j.atmosenv.2011.06.056

Avnery, S, Mauzerall, DL, Liu, JF and **Horowitz, LW.** 2011. Global crop yield reductions due to surface ozone exposure: 1. Year 2000 crop production losses and economic damage. *Atmos Environ* **45**(13): 2284–2296. DOI: https://doi.org/10.1016/j.atmosenv.2010.11.045

Bak, J, Kim, JH, Liu, X, Chance, K and **Kim, J.** 2013. Evaluation of ozone profile and tropospheric ozone retrievals from GEMS and OMI spectra. *Atmos Meas Tech* **6**(2): 239–249. DOI: https://doi.org/10.5194/amt-6-239-2013

Baker, KR, Woody, MC, Tonnesen, GS, Hutzell, W, Pye, HOT, Beaver, MR, Pouliot, G and **Pierce, T.** 2016. Contribution of regional-scale fire events to ozone and $PM_{2.5}$ air quality estimated by photochemical modeling approaches. *Atmos Environ* **140**: 539–554. DOI: https://doi.org/10.1016/j.atmosenv.2016.06.032

Barnes, EA, Fiore, AM and **Horowitz, LW.** 2016. Detection of trends in surface ozone in the presence of climate variability. *J Geophys Res Atmos* **121**(10): 6112–6129. DOI: https://doi.org/10.1002/2015jd024397

Baylon, P, Jaffe, DA, Wigder, NL, Gao, H and **Hee, J.** 2015. Ozone enhancement in western US wildfire plumes at the Mt. Bachelor Observatory: The role of NO_x. *Atmos Environ* **109**: 297–304. DOI: https://doi.org/10.1016/j.atmosenv.2014.09.013

Baylon, PM, Jaffe, DA, Pierce, RB and **Gustin, MS.** 2016. Interannual variability in baseline ozone and its relationship to surface ozone in the western US. *Environ Sci Technol* **50**(6): 2994–3001. DOI: https://doi.org/10.1021/acs.est.6b00219

Bell, ML, McDermott, A, Zeger, SL, Samet, JM and **Dominici, F.** 2004. Ozone and short-term mortality in 95 US urban communities, 1987–2000. *JAMA* **292**(19): 2372–2378. DOI: https://doi.org/10.1001/jama.292.19.2372

Bloomer, BJ, Vinnikov, KY and **Dickerson, RR.** 2010. Changes in seasonal and diurnal cycles of ozone and temperature in the eastern US. *Atmos Environ* **44**(21–22): 2543–2551. DOI: https://doi.org/10.1016/j.atmosenv.2010.04.031

Briggs, NL, Jaffe, DA, Gao, HL, Hee, JR, Baylon, PM, Zhang, Q, Zhou, S, Collier, SC, Sampson, PD and **Cary, RA.** 2016. Particulate matter, ozone, and nitrogen species in aged wildfire plumes observed at the Mount Bachelor Observatory. *Aerosol Air Qual Res* **16**(12): 3075–3087. DOI: https://doi.org/10.4209/aaqr.2016.03.0120

Brioude, J, Cooper, OR, Trainer, M, Ryerson, TB, Holloway, JS, Baynard, T, Peischl, J, Warneke, C, Neuman, JA, De Gouw, J, Stohl, A, Eckhardt, S, Frost, GJ, McKeen, SA, Hsie, EY, Fehsenfeld, FC and **Nedelec, P.** 2007. Mixing between a stratospheric intrusion and a biomass burning plume. *Atmos Chem Phys* **7**(16): 4229–4235. DOI: https://doi.org/10.5194/acp-7-4229-2007

Brown-Steiner, B, Hess, PG and **Lin, MY.** 2015. On the capabilities and limitations of GCCM simulations of summertime regional air quality: A diagnostic analysis of ozone and temperature simulations in the US using CESM CAM-Chem. *Atmos Environ* **101**: 134–148. DOI: https://doi.org/10.1016/j.atmosenv.2014.11.001

Butler, TM, Lawrence, MG, Taraborrelli, D and **Lelieveld, J.** 2011. Multi-day ozone production potential of volatile organic compounds calculated with a tagging approach. *Atmos Environ* **45**(24): 4082–4090. DOI: https://doi.org/10.1016/j.atmosenv.2011.03.040

Byun, D and **Schere, KL.** 2006. Review of the governing equations, computational algorithms, and other components of the models-3 Community Multiscale Air Quality (CMAQ) modeling system. *Applied Mechanics Reviews* **59**(1–6): 51–77. DOI: https://doi.org/10.1115/1.2128636

California Air Resources Board (CARB). 2011. Exceptional Events Demonstration for 1-Hour Ozone Exceedances in the Sacramento Regional Nonattainment Area Due to 2008 Wildfires. California Air Resources Board. Available at: https://www.arb.ca.gov/desig/excevents/firemain.pdf. Accessed October 27, 2017.

Camalier, L, Cox, W and **Dolwick, P.** 2007. The effects of meteorology on ozone in urban areas and their use in assessing ozone trends. *Atmos Environ* **41**(33): 7127–7137. DOI: https://doi.org/10.1016/j.atmosenv.2007.04.061

Cohan, DS, Hakami, A, Hu, YT and **Russell, AG.** 2005. Nonlinear response of ozone to emissions: Source apportionment and sensitivity analysis. *Environ Sci Technol* **39**(17): 6739–6748. DOI: https://doi.org/10.1021/es048664m

Cohan, DS and **Napelenok, SL.** 2011. Air quality response modeling for decision support. *Atmosphere* **2**(3): 407–425. DOI: https://doi.org/10.3390/atmos2030407

Collet, S, Minoura, H, Kidokoro, T, Sonoda, Y, Kinugasa, Y, Karamchandani, P, Johnson, J, Shah, T, Jung, J and **DenBleyker, A.** 2014. Future year ozone source attribution modeling studies for the eastern and western United States. *J Air Waste Manage Assoc* **64**(10): 1174–1185. DOI: https://doi.org/10.1080/10962247.2014.936629

Cooper, O, Forster, C, Parrish, D, Dunlea, E, Hubler, G, Fehsenfeld, F, Holloway, J, Oltmans, S, Johnson, B, Wimmers, A and **Horowitz, L.** 2004a. On the life cycle of a stratospheric intrusion and its dispersion into polluted warm conveyor belts. *J Geophys Res Atmos* **109**(D23): S09. DOI: https://doi.org/10.1029/2003jd004006

Cooper, OR, Forster, C, Parrish, D, Trainer, M, Dunlea, E, Ryerson, T, Hubler, G, Fehsenfeld, F, Nicks, D, Holloway, J, de Gouw, J, Warneke, C, Roberts, JM, Flocke, F and **Moody, J.** 2004b. A case study of transpacific warm conveyor belt transport: Influence of merging airstreams on trace gas import to North America. *J Geophys Res Atmos* **109**(D23): S08. DOI: https://doi.org/10.1029/2003jd003624

Cooper, OR, Gao, R-S, Tarasick, D, Leblanc, T and **Sweeney, C.** 2012. Long-term ozone trends at rural ozone monitoring sites across the United States, 1990–2010. *J Geophys Res Atmos* **117**(D22): 307. DOI: https://doi.org/10.1029/2012jd018261

Cooper, OR, Langford, AO, Parrish, DD and **Fahey, DW.** 2015. Challenges of a lowered US ozone standard. *Science* **348**(6239): 1096–1097. DOI: https://doi.org/10.1126/science.aaa5748

Cooper, OR, Oltmans, SJ, Johnson, BJ, Brioude, J, Angevine, W, Trainer, M, Parrish, DD, Ryerson, TR, Pollack, I, Cullis, PD, Ives, MA, Tarasick, DW, Al-Saadi, J and **Stajner, I.** 2011. Measurement of western U.S. baseline ozone from the surface to the tropopause and assessment of downwind impact regions. *J Geophys Res* **116**(D00): V03. DOI: https://doi.org/10.1029/2011jd016095

Cooper, OR, Parrish, DD, Ziemke, J, Balashov, NV, Cupeiro, M, Galbally, IE, Gilge, S, Horowitz, L, Jensen, NR and **Lamarque, J-F.** 2014. Global distribution and trends of tropospheric ozone: An observation-based review. *Elementa* **2**(29). DOI: https://doi.org/10.12952/journal.elementa.000029

Dennison, PE, Brewer, SC, Arnold, JD and **Moritz, MA.** 2014. Large wildfire trends in the western United States, 1984–2011. *Geophys Res Lett* **41**(8): 2928–2933. DOI: https://doi.org/10.1002/2014gl059576

Deser, C, Knutti, R, Solomon, S and **Phillips, AS.** 2012. Communication of the role of natural variability in future North American climate. *Nature Climate Change* **2**: 775. DOI: https://doi.org/10.1038/nclimate1562

Dolwick, P, Akhtar, F, Baker, KR, Possiel, N, Simon, H and **Tonnesen, G.** 2015. Comparison of background ozone estimates over the western United States based on two separate model methodologies. *Atmos Environ* **109**: 282–296. DOI: https://doi.org/10.1016/j.atmosenv.2015.01.005

Dreessen, J, Sullivan, J and **Delgado, R.** 2016. Observations and impacts of transported Canadian wildfire smoke on ozone and aerosol air quality in the Maryland region on June 9–12, 2015. *J Air Waste Manage Assoc* **66**(9): 842–862. DOI: https://doi.org/10.1080/10962247.2016.1161674

Dunker, AM. 1981. Efficient calculation of sensitivity coefficients for complex atmospheric models. *Atmos Environ* **15**(7): 1155–1161. DOI: https://doi.org/10.1016/0004-6981(81)90305-x

Dunker, AM, Koo, B and **Yarwood, G.** 2017. Contributions of foreign, domestic and natural emissions to US ozone estimated using the path-integral method in CAMx nested within GEOS-Chem. *Atmos Chem Phys* **17**(20): 12553–12571. DOI: https://doi.org/10.5194/acp-17-12553-2017

Eastham, SD and **Jacob, DJ.** 2017. Limits on the ability of global Eulerian models to resolve intercontinental transport of chemical plumes. *Atmos Chem Phys* **17**(4): 2543–2553. DOI: https://doi.org/10.5194/acp-17-2543-2017

Emery, C, Jung, J, Downey, N, Johnson, J, Jimenez, M, Yarwood, G and **Morris, R.** 2012. Regional and global modeling estimates of policy relevant background ozone over the United States. *Atmos Environ* **47**: 206–217. DOI: https://doi.org/10.1016/j.atmosenv.2011.11.012

Emmons, LK, Hess, PG, Lamarque, JF and **Pfister, GG.** 2012. Tagged ozone mechanism for MOZART-4, CAM-chem and other chemical transport models. *Geosci Model Dev* **5**(6): 1531–1542. DOI: https://doi.org/10.5194/gmd-5-1531-2012

Fine, R, Miller, MB, Burley, J, Jaffe, DA, Pierce, RB, Lin, MY and **Gustin, MS.** 2015. Variability and sources of surface ozone at rural sites in Nevada, USA: Results from two years of the Nevada Rural Ozone Initiative. *Sci Total Environ* **530**: 471–482. DOI: https://doi.org/10.1016/j.scitotenv.2014.12.027

Fiore, AM, Dentener, FJ, Wild, O, Cuvelier, C, Schultz, MG, Hess, P, Textor, C, Schulz, M, Doherty, RM, Horowitz, LW, MacKenzie, IA, Sanderson, MG, Shindell, DT, Stevenson, DS, Szopa, S, Van Dingenen, R, Zeng, G, Atherton, C, Bergmann, D, Bey, I, Carmichael, G, Collins, WJ, Duncan, BN, Faluvegi, G, Folberth, G, Gauss, M, Gong, S, Hauglustaine, D, Holloway, T, Isaksen, ISA, Jacob, DJ, Jonson, JE, Kaminski, JW, Keating, TJ, Lupu, A, Marmer, E, Montanaro, V, Park, RJ, Pitari, G, Pringle, KJ, Pyle, JA, Schroeder, S, Vivanco, MG, Wind, P, Wojcik, G, Wu, S and **Zuber, A.** 2009. Multimodel estimates of intercontinental source-receptor relationships for ozone pollution. *J Geophys Res Atmos* **114**(D4). DOI: https://doi.org/10.1029/2008jd010816

Fiore, AM, Jacob, DJ, Bey, I, Yantosca, RM, Field, BD, Fusco, AC and **Wilkinson, JG.** 2002. Background ozone over the United States in summer: Origin, trend, and contribution to pollution episodes. *J Geophys Res Atmos* **107**(D15). DOI: https://doi.org/10.1029/2001jd000982

Fiore, AM, Jacob, DJ, Liu, H, Yantosca, RM, Fairlie, TD and **Li, Q.** 2003. Variability in surface ozone background over the United States: Implications for air quality policy. *J Geophys Res* **108**(D24): 4787. DOI: https://doi.org/10.1029/2003jd003855

Fiore, AM, Naik, V and **Leibensperger, EM.** 2015. Air quality and climate connections. *J Air Waste Manage Assoc* **65**(6): 645–685. DOI: https://doi.org/10.1080/10962247.2015.1040526

Fiore, AM, Oberman, JT, Lin, MY, Zhang, L, Clifton, OE, Jacob, DJ, Naik, V, Horowitz, LW, Pinto, JP and **Milly, GP.** 2014a. Estimating North American background ozone in U.S. surface air with two independent global models: Variability, uncertainties, and recommendations. *Atmos Environ* **96**: 284–300. DOI: https://doi.org/10.1016/j.atmosenv.2014.07.045

Fiore, AM, Pierce, RB, Dickerson, RR and **Lin, M.** 2014b. Detecting and attributing episodic high background ozone events. *EM*, 22–28. February 2014.

Fiore, AM, West, JJ, Horowitz, LW, Naik, V and **Schwarzkopf, MD.** 2008. Characterizing the tropospheric ozone response to methane emission controls and the benefits to climate and air quality. *J Geophys Res Atmos* **113**(D8). DOI: https://doi.org/10.1029/2007jd009162

Foley, KM, Hogrefe, C, Pouliot, G, Possiel, N, Roselle, SJ, Simon, H and **Timin, B.** 2015. Dynamic evaluation of CMAQ part I: Separating the effects of changing emissions and changing meteorology on ozone levels between 2002 and 2005 in the eastern US. *Atmos Environ* **103**: 247–255. DOI: https://doi.org/10.1016/j.atmosenv.2014.12.038

Fusco, AC and **Logan, JA.** 2003. Analysis of 1970–1995 trends in tropospheric ozone at Northern Hemisphere midlatitudes with the GEOS-CHEM model. *J Geophys Res Atmos* **108**(D15). DOI: https://doi.org/10.1029/2002jd002742

Galmarini, S, Koffi, B, Solazzo, E, Keating, T, Hogrefe, C, Schulz, M, Benedictow, A, Griesfeller, JJ, Janssens-Maenhout, G, Carmichael, G, Fu, J and **Dentener, F.** 2017. Technical note: Coordination and harmonization of the multi-scale, multi-model activities HTAP2, AQMEII3, and MICS-Asia3: Simulations, emission inventories, boundary conditions, and model output formats. *Atmos Chem Phys* **17**(2): 1543–1555. DOI: https://doi.org/10.5194/acp-17-1543-2017

Gong, X, Nair, U, Kaulfus, A and **Jaffe, DA.** 2017. Quantifying O_3 impacts in urban areas due to wildfires using a Generalized Additive Model. *Environ Sci Technol* **1**(22): 13216–13223. DOI: https://doi.org/10.1021/acs.est.7b03130

Gratz, LE, Jaffe, DA and **Hee, JR.** 2015. Causes of increasing ozone and decreasing carbon monoxide in springtime at the Mt. Bachelor Observatory from 2004 to 2013. *Atmos Environ* **109**: 323–330. DOI: https://doi.org/10.1016/j.atmosenv.2014.05.076

Grewe, V, Tsati, E and **Hoor, P.** 2010. On the attribution of contributions of atmospheric trace gases to emissions in atmospheric model applications. *Geosci Model Dev* **3**(2): 487–499. DOI: https://doi.org/10.5194/gmd-3-487-2010

Grewe, V, Tsati, E, Mertens, M, Fromming, C and **Jockel, P.** 2017. Contribution of emissions to concentrations: The TAGGING 1.0 submodel based on the Modular Earth Submodel System (MESSy 2.52). *Geosci Model Dev* **10**(7): 2615–2633. DOI: https://doi.org/10.5194/gmd-10-2615-2017

Guo, JJ, Fiore, AM, Murray, LT, Jaffe, DA, Schnell, JL, Moore, T and **Milly, G.** 2018. Average versus high surface ozone levels over the continental U.S.A.: Model bias, background influences, and interannual variability. *Atmos Chem Phys Discuss* **2018**: 1–31. DOI: https://doi.org/10.5194/acp-2018-115

Guo, YX, Liu, JF, Mauzerall, DL, Li, XY, Horowitz, LW, Tao, W and **Tao, S.** 2017. Long-Lived Species Enhance Summertime Attribution of North American Ozone to Upwind Sources. *Environ Sci Technol*

51(9): 5017–5025. DOI: https://doi.org/10.1021/acs.est.6b05664

Gustin, MS, Fine, R, Miller, M, Jaffe, D and **Burley, J.** 2015. The Nevada Rural Ozone Initiative (NVROI): Insights to understanding air pollution in complex terrain. *Sci Total Environ* **530**: 455–470. DOI: https://doi.org/10.1016/j.scitotenv.2015.03.046

Hakami, A, Odman, MT and **Russell, AG.** 2004. Nonlinearity in atmospheric response: A direct sensitivity analysis approach. *J Geophys Res Atmos* **109**(D15): 12. DOI: https://doi.org/10.1029/2003jd004502

Hassler, B, McDonald, BC, Frost, GJ, Borbon, A, Carslaw, DC, Civerolo, K, Granier, C, Monks, PS, Monks, S, Parrish, DD, Pollack, IB, Rosenlof, KH, Ryerson, TB, von Schneidemesser, E and **Trainer, M.** 2016. Analysis of long-term observations of NO_x and CO in megacities and application to constraining emissions inventories. *Geophys Res Lett* **43**(18): 9920–9930. DOI: https://doi.org/10.1002/2016gl069894

He, H, Tarasick, DW, Hocking, WK, Carey-Smith, TK, Rochon, Y, Zhang, J, Makar, PA, Osman, M, Brook, J, Moran, MD, Jones, DBA, Mihele, C, Wei, JC, Osterman, G, Argall, PS, McConnell, J and **Bourqui, MS.** 2011. Transport analysis of ozone enhancement in Southern Ontario during BAQS-Met. *Atmos Chem Phys* **11**(6): 2569–2583. DOI: https://doi.org/10.5194/acp-11-2569-2011

Hemispheric Transport of Air Pollution (HTAP). 2010. *Hemispheric Transport of Air Pollution 2010, Part A: Ozone and Particulate Matter.* Task Force on Hemispheric Transport of Air Pollution. Dentener, F, Keating, T and Akimoto, H (eds.). Air Pollution Studies, No. 17. Geneva: United Nations Economic Commission for Europe.

Herron-Thorpe, FL, Mount, GH, Emmons, LK, Lamb, BK, Jaffe, DA, Wigder, NL, Chung, SH, Zhang, R, Woelfle, MD and **Vaughan, JK.** 2014. Air quality simulations of wildfires in the Pacific Northwest evaluated with surface and satellite observations during the summers of 2007 and 2008. *Atmos Chem Phys* **14**(22): 12533–12551. DOI: https://doi.org/10.5194/acp-14-12533-2014

Hoesly, RM, Smith, SJ, Feng, L, Klimont, Z, Janssens-Maenhout, G, Pitkanen, T, Seibert, JJ, Vu, L, Andres, RJ, Bolt, RM, Bond, TC, Dawidowski, L, Kholod, N, Kurokawa, JI, Li, M, Liu, L, Lu, Z, Moura, MCP, O'Rourke, PR and **Zhang, Q.** 2018. Historical (1750–2014) anthropogenic emissions of reactive gases and aerosols from the Community Emission Data System (CEDS). *Geosci Model Dev* **11**: 369–408. DOI: https://doi.org/10.5194/gmd-11-369-2018

Hogrefe, C, Liu, P, Pouliot, G, Mathur, R, Roselle, S, Flemming, J, Lin, M and **Park, RJ.** 2018. Impacts of different characterizations of large-scale background on simulated regional-scale ozone over the continental United States. *Atmos Chem Phys* **18**: 3839–3864. DOI: https://doi.org/10.5194/acp-18-3839-2018

Huang, M, Bowman, KW, Carmichael, GR, Lee, M, Chai, TF, Spak, SN, Henze, DK, Darmenov, AS and **da Silva, AM.** 2015. Improved western US background ozone estimates via constraining nonlocal and local source contributions using Aura TES and OMI observations. *J Geophys Res Atmos* **120**(8): 3572–3592. DOI: https://doi.org/10.1002/2014jd022993

Huang, M, Bowman, KW, Carmichael, GR, Pierce, RB, Worden, HM, Luo, M, Cooper, OR, Pollack, IB, Ryerson, TB and **Brown, SS.** 2013a. Impact of Southern California anthropogenic emissions on ozone pollution in the mountain states: Model analysis and observational evidence from space. *J Geophys Res Atmos* **118**(22): 12784–12803. DOI: https://doi.org/10.1002/2013jd020205

Huang, M, Carmichael, GR, Adhikary, B, Spak, SN, Kulkarni, S, Cheng, YF, Wei, C, Tang, Y, Parrish, DD, Oltmans, SJ, D'Allura, A, Kaduwela, A, Cai, C, Weinheimer, AJ, Wong, M, Pierce, RB, Al-Saadi, JA, Streets, DG and **Zhang, Q.** 2010. Impacts of transported background ozone on California air quality during the ARCTAS-CARB period – a multi-scale modeling study. *Atmos Chem Phys* **10**(14): 6947–6968. DOI: https://doi.org/10.5194/acp-10-6947-2010

Huang, M, Carmichael, GR, Chai, T, Pierce, RB, Oltmans, SJ, Jaffe, DA, Bowman, KW, Kaduwela, A, Cai, C, Spak, SN, Weinheimer, AJ, Huey, LG and **Diskin, GS.** 2013b. Impacts of transported background pollutants on summertime western US air quality: Model evaluation, sensitivity analysis and data assimilation. *Atmos Chem Phys* **13**(1): 359–391. DOI: https://doi.org/10.5194/acp-13-359-2013

Huang, M, Carmichael, GR, Pierce, RB, Jo, DS, Park, RJ, Flemming, J, Emmons, LK, Bowman, KW, Henze, DK, Davila, Y, Sudo, K, Jonson, JE, Tronstad Lund, M, Janssens-Maenhout, G, Dentener, FJ, Keating, TJ, Oetjen, H and **Payne, VH.** 2017. Impact of intercontinental pollution transport on North American ozone air pollution: An HTAP phase 2 multi-model study. *Atmos Chem Phys* **17**(9): 5721–5750. DOI: https://doi.org/10.5194/acp-17-5721-2017

Jacob, DJ, Crawford, JH, Maring, H, Clarke, AD, Dibb, JE, Emmons, LK, Ferrare, RA, Hostetler, CA, Russell, PB, Singh, HB, Thompson, AM, Shaw, GE, McCauley, E, Pederson, JR and **Fisher, JA.** 2010. The Arctic Research of the composition of the troposphere from Aircraft and Satellites (ARCTAS) mission: Design, execution, and first results. *Atmos Chem Phys* **10**(11): 5191–5212. DOI: https://doi.org/10.5194/acp-10-5191-2010

Jacob, DJ, Logan, JA and **Murti, PP.** 1999. Effect of rising Asian emissions on surface ozone in the United States. *Geophys Res Lett* **26**(14): 2175–2178. DOI: https://doi.org/10.1029/1999gl900450

Jaeglé, L, Steinberger, L, Martin, RV and **Chance, K.** 2005. Global partitioning of NO_x sources using satellite observations: Relative roles of fossil fuel combustion, biomass burning and soil emissions.

Faraday Discussions **130**: 407–423. DOI: https://doi.org/10.1039/b502128f

Jaffe, D. 2011. Relationship between surface and free tropospheric ozone in the western U.S. *Environ Sci Technol* **45**(2): 432–438. DOI: https://doi.org/10.1021/es1028102

Jaffe, D, Bertschi, I, Jaeglé, L, Novelli, P, Reid, JS, Tanimoto, H, Vingarzan, R and **Westphal, DL.** 2004. Long-range transport of Siberian biomass burning emissions and impact on surface ozone in western North America. *Geophys Res Lett* **31**(L16): 106. DOI: https://doi.org/10.1029/2004GL020093

Jaffe, D, Chand, D, Hafner, W, Westerling, A and **Spracklen, D.** 2008. Influence of fires on O_3 concentrations in the western US. *Environ Sci Technol* **42**: 5885–5891. DOI: https://doi.org/10.1021/es800084k

Jaffe, D, Prestbo, E, Swartzendruber, P, Weiss-Penzias, P, Kato, S, Takami, A, Hatakeyama, S and **Kajii, Y.** 2005. Export of atmospheric mercury from Asia. *Atmos Environ* **39**(17): 3029–3038. DOI: https://doi.org/10.1016/j.atmosenv.2005.01.030

Jaffe, DA, Wigder, N, Downey, N, Pfister, G, Boynard, A and **Reid, SB.** 2013. Impact of wildfires on ozone exceptional events in the western US. *Environ Sci Technol* **47**(19): 11065–11072. DOI: https://doi.org/10.1021/es402164f

Jaffe, DA and **Wigder, NL.** 2012. Ozone production from wildfires: A critical review. *Atmos Environ* **51**: 1–10. DOI: https://doi.org/10.1016/j.atmosenv.2011.11.063

Jaffe, DA and **Zhang, L.** 2017. Meteorological anomalies lead to elevated O_3 in the western U.S. in June 2015. *Geophys Res Lett* **44**(4): 1990–1997. DOI: https://doi.org/10.1002/2016GL072010

Karamchandani, P, Morris, R, Wentland, A, Shah, T, Reid, S and **Lester, J.** 2017. Dynamic Evaluation of Photochemical Grid Model Response to Emission Changes in the South Coast Air Basin in California. *Atmosphere* **8**(8). DOI: https://doi.org/10.3390/atmos8080145

Knote, C, Tuccella, P, Curci, G, Emmons, L, Orlando, JJ, Madronich, S, Baro, R, Jimenez-Guerrero, P, Luecken, D, Hogrefe, C, Forkel, R, Werhahn, J, Hirtl, M, Perez, JL, San Jose, R, Giordano, L, Brunner, D, Yahya, K and **Zhang, Y.** 2015. Influence of the choice of gas-phase mechanism on predictions of key gaseous pollutants during the AQMEII phase-2 intercomparison. *Atmos Environ* **115**: 553–568. DOI: https://doi.org/10.1016/j.atmosenv.2014.11.066

Knowland, KE, Ott, LE, Duncan, BN and **Wargan, K.** 2017. Stratospheric Intrusion-Influenced Ozone Air Quality Exceedances Investigated in the NASA MERRA-2 Reanalysis. *Geophys Res Lett* **44**(20): 10691–10701. DOI: https://doi.org/10.1002/2017gl074532

Koumoutsaris, S and **Bey, I.** 2012. Can a global model reproduce observed trends in summertime surface ozone levels? *Atmos Chem Phys* **12**(15): 6983–6998. DOI: https://doi.org/10.5194/acp-12-6983-2012

Krotkov, NA, McLinden, CA, Li, C, Lamsal, LN, Celarier, EA, Marchenko, SV, Swartz, WH, Bucsela, EJ, Joiner, J, Duncan, BN, Boersma, KF, Veefkind, JP, Levelt, PF, Fioletov, VE, Dickerson, RR, He, H, Lu, ZF and **Streets, DG.** 2016. Aura OMI observations of regional SO_2 and NO_2 pollution changes from 2005 to 2015. *Atmos Chem Phys* **16**(7): 4605–4629. DOI: https://doi.org/10.5194/acp-16-4605-2016

Kuang, S, Newchurch, MJ, Burris, J, Wang, LH, Knupp, K and **Huang, GY.** 2012. Stratosphere-to-troposphere transport revealed by ground-based lidar and ozonesonde at a midlatitude site. *J Geophys Res Atmos* **117**. DOI: https://doi.org/10.1029/2012jd017695

Kwok, RHF, Baker, KR, Napelenok, SL and **Tonnesen, GS.** 2015. Photochemical grid model implementation and application of VOC, NO_x, and O-3 source apportionment. *Geosci Model Dev* **8**(1): 99–114. DOI: https://doi.org/10.5194/gmd-8-99-2015

Lamarque, JF, Bond, TC, Eyring, V, Granier, C, Heil, A, Klimont, Z, Lee, D, Liousse, C, Mieville, A, Owen, B, Schultz, MG, Shindell, D, Smith, SJ, Stehfest, E, Van Aardenne, J, Cooper, OR, Kainuma, M, Mahowald, N, McConnell, JR, Naik, V, Riahi, K and **van Vuuren, DP.** 2010. Historical (1850–2000) gridded anthropogenic and biomass burning emissions of reactive gases and aerosols: Methodology and application. *Atmos Chem Phys* **10**(15): 7017–7039. DOI: https://doi.org/10.5194/acp-10-7017-2010

Lamsal, LN, Duncan, BN, Yoshida, Y, Krotkov, NA, Pickering, KE, Streets, DG and **Lu, ZF.** 2015. U.S. NO_2 trends (2005–2013): EPA Air Quality System (AQS) data versus improved observations from the Ozone Monitoring Instrument (OMI). *Atmos Environ* **110**: 130–143. DOI: https://doi.org/10.1016/j.atmosenv.2015.03.055

Landrigan, PJ, Fuller, R, Acosta, NJR, Adeyi, O, Arnold, R, Basu, N, Balde, AB, Bertollini, R, Bose-O'Reilly, S, Boufford, JI, Breysse, PN, Chiles, T, Mahidol, C, Coll-Seck, AM, Cropper, ML, Fobil, J, Fuster, V, Greenstone, M, Haines, A, Hanrahan, D, Hunter, D, Khare, M, Krupnick, A, Lanphear, B, Lohani, B, Martin, K, Mathiasen, KV, McTeer, MA, Murray, CJL, Ndahimananjara, JD, Perera, F, Potocnik, J, Preker, AS, Ramesh, J, Rockstrom, J, Salinas, C, Samson, LD, Sandilya, K, Sly, PD, Smith, KR, Steiner, A, Stewart, RB, Suk, WA, van Schayck, OCP, Yadama, GN, Yumkella, K and **Zhong, M.** 2018. The Lancet Commission on pollution and health. *Lancet* **391**(10119): 462–512. DOI: https://doi.org/10.1016/s0140-6736(17)32345-0

Langford, AO, Aikin, KC, Eubank, CS and **Williams, EJ.** 2009. Stratospheric contribution to high surface ozone in Colorado during springtime. *Geophys Res Lett* **36**(L12): 801. DOI: https://doi.org/10.1029/2009gl038367

Langford, AO, Alvarez, RJ, Brioude, J, Evan, S, Iraci, LT, Kirgis, G, Kuang, S, Leblanc, T, Newchurch, MJ, Pierce, RB, Senff, CJ and **Yates, EL.** 2018. Coordinated profiling of stratospheric intrusions and transported pollution by the Tropospheric Ozone Lidar

Network (TOLNet) and NASA Alpha Jet experiment (AJAX): Observations and comparison to HYSPLIT, RAQMS, and FLEXPART. *Atmos Environ* **174**(Supplement C): 1–14. DOI: https://doi.org/10.1016/j.atmosenv.2017.11.031

Langford, AO, Alvarez, RJ, II, Brioude, J, Fine, R, Gustin, MS, Lin, MY, Marchbanks, RD, Pierce, RB, Sandberg, SP, Senff, CJ, Weickmann, AM and **Williams, EJ.** 2017. Entrainment of stratospheric air and Asian pollution by the convective boundary layer in the southwestern U.S. *J Geophys Res Atmos* **122**: 1312–1337. DOI: https://doi.org/10.1002/2016JD025987

Langford, AO, Brioude, J, Cooper, OR, Senff, CJ, Alvarez, RJ, Hardesty, RM, Johnson, BJ and **Oltmans, SJ.** 2012. Stratospheric influence on surface ozone in the Los Angeles area during late spring and early summer of 2010. *J Geophys Res Atmos* **117**(D00): V06. DOI: https://doi.org/10.1029/2011jd016766

Langford, AO, Pierce, RB and **Schultz, PJ.** 2015b. Stratospheric intrusions, the Santa Ana winds, and wildland fires in Southern California. *Geophys Res Lett* **42**(14): 6091–6097. DOI: https://doi.org/10.1002/2015gl064964

Langford, AO, Senff, CJ, Alvarez, RJ, Brioude, J, Cooper, OR, Holloway, JS, Lin, MY, Marchbanks, RD, Pierce, RB, Sandberg, SP, Weickmann, AM and **Williams, EJ.** 2015a. An overview of the 2013 Las Vegas Ozone Study (LVOS): Impact of stratospheric intrusions and long-range transport on surface air quality. *Atmos Environ* **109**: 305–322. DOI: https://doi.org/10.1016/j.atmosenv.2014.08.040

Lapina, K, Henze, DK, Milford, JB, Huang, M, Lin, MY, Fiore, AM, Carmichael, G, Pfister, GG and **Bowman, K.** 2014. Assessment of source contributions to seasonal vegetative exposure to ozone in the US. *J Geophys Res Atmos* **119**(1): 324–340. DOI: https://doi.org/10.1002/2013jd020905

Lapina, K, Henze, DK, Milford, JB and **Travis, K.** 2016. Impacts of foreign, domestic, and state-level emissions on ozone-induced vegetation loss in the United States. *Environ Sci Technol* **50**(2): 806–813. DOI: https://doi.org/10.1021/acs.est.5b04887

Lefohn, AS, Emery, C, Shadwick, D, Wernli, H, Jung, J and **Oltmans, SJ.** 2014. Estimates of background surface ozone concentrations in the United States based on model-derived source apportionment. *Atmos Environ* **84**: 275–288. DOI: https://doi.org/10.1016/j.atmosenv.2013.11.033

Lefohn, AS, Wernli, H, Shadwick, D, Oltmans, SJ and **Shapiro, M.** 2012. Quantifying the importance of stratospheric-tropospheric transport on surface ozone concentrations at high- and low-elevation monitoring sites in the United States. *Atmos Environ* **62**: 646–656. DOI: https://doi.org/10.1016/j.atmosenv.2012.09.004

Lin, M, Fiore, AM, Cooper, OR, Horowitz, LW, Langford, AO, Levy, H, Johnson, BJ, Naik, V, Oltmans, SJ and **Senff, CJ.** 2012a. Springtime high surface ozone events over the western United States: Quantifying the role of stratospheric intrusions. *J Geophys Res Atmos* **117**(D00): V22. DOI: https://doi.org/10.1029/2012jd018151

Lin, M, Fiore, AM, Horowitz, LW, Cooper, OR, Naik, V, Holloway, J, Johnson, BJ, Middlebrook, AM, Oltmans, SJ, Pollack, IB, Ryerson, TB, Warner, JX, Wiedinmyer, C, Wilson, J and **Wyman, B.** 2012b. Transport of Asian ozone pollution into surface air over the western United States in spring. *J Geophys Res Atmos* **117**(D00): V07. DOI: https://doi.org/10.1029/2011JD016961

Lin, M, Holloway, T, Carmichael, GR and **Fiore, AM.** 2010. Quantifying pollution inflow and outflow over East Asia in spring with regional and global models. *Atmos Chem Phys* **10**(9): 4221–4239. DOI: https://doi.org/10.5194/acp-10-4221-2010

Lin, MY, Fiore, AM, Horowitz, LW, Langford, AO, Oltmans, SJ, Tarasick, D and **Rieder, HE.** 2015b. Climate variability modulates western US ozone air quality in spring via deep stratospheric intrusions. *Nat Commun* **6**(7105). DOI: https://doi.org/10.1038/ncomms8105

Lin, MY, Horowitz, LW, Cooper, OR, Tarasick, D, Conley, S, Iraci, LT, Johnson, B, Leblanc, T, Petropavlovskikh, I and **Yates, EL.** 2015a. Revisiting the evidence of increasing springtime ozone mixing ratios in the free troposphere over western North America. *Geophys Res Lett* **42**(20): 8719–8728. DOI: https://doi.org/10.1002/2015gl065311

Lin, M, Horowitz, LW, Oltmans, SJ, Fiore, AM and **Fan, S.** 2014. Tropospheric ozone trends at Mauna Loa Observatory tied to decadal climate variability. *Nat Geosci* **7**: 136–143. DOI: https://doi.org/10.1038/ngeo2066

Lin, M, Horowitz, LW, Payton, R, Fiore, AM and **Tonnesen, GS.** 2017. US surface ozone trends and extremes from 1980 to 2014: Quantifying the roles of rising Asian emissions, domestic controls, wildfires, and climate *Atmos Chem Phys* **17**: 2943–2970. DOI: https://doi.org/10.5194/acp-17-2943-2017

Lippmann, M. 1993. Health-effects of tropospheric ozone – review of recent research findings and their implications to ambient air-quality standards. *J Expo Anal Env Epid* **3**(1): 103–129.

Liu, X, Bhartia, PK, Chance, K, Spurr, RJD and **Kurosu, TP.** 2010. Ozone profile retrievals from the Ozone Monitoring Instrument. *Atmos Chem Phys* **10**: 2521–2537. DOI: https://doi.org/10.5194/acp-10-2521-2010

Liu, XX, Zhang, Y, Huey, LG, Yokelson, RJ, Wang, Y, Jimenez, JL, Campuzano-Jost, P, Beyersdorf, AJ, Blake, DR, Choi, Y, St Clair, JM, Crounse, JD, Day, DA, Diskin, GS, Fried, A, Hall, SR, Hanisco, TF, King, LE, Meinardi, S, Mikoviny, T, Palm, BB, Peischl, J, Perring, AE, Pollack, IB, Ryerson, TB, Sachse, G, Schwarz, JP, Simpson, IJ, Tanner, DJ, Thornhill, KL, Ullmann, K, Weber, RJ, Wennberg, PO, Wisthaler, A, Wolfe, GM and **Ziemba, LD.** 2016. Agricultural fires in the southeastern US during SEAC^{4}RS: Emissions of trace gases and particles

and evolution of ozone, reactive nitrogen, and organic aerosol. *J Geophys Res Atmos* **121**(12): 7383–7414. DOI: https://doi.org/10.1002/2016jd025040

Logan, JA. 1999. An analysis of ozonesonde data for the troposphere: Recommendations for testing 3-D models and development of a gridded climatology for tropospheric ozone. *J Geophys Res Atmos* **104**(D13): 16115–16149. DOI: https://doi.org/10.1029/1998jd100096

Lu, X, Zhang, L, Yue, X, Zhang, JC, Jaffe, DA, Stohl, A, Zhao, YH and **Shao, JY.** 2016. Wildfire influences on the variability and trend of summer surface ozone in the mountainous western United States. *Atmos Chem Phys* **16**(22): 14687–14702. DOI: https://doi.org/10.5194/acp-16-14687-2016

McCarty, JL, Justice, CO and **Korontzi, S.** 2007. Agricultural burning in the Southeastern United States detected by MODIS. *Remote Sens Environ* **108**(2): 151–162. DOI: https://doi.org/10.1016/j.rse.2006.03.020

McClure, CD and **Jaffe, DA.** 2018. U.S. particulate matter air quality improves except in wildfire-prone areas. *PNAS*. DOI: https://doi.org/10.1073/pnas.1804353115

McDonald-Buller, EC, Allen, DT, Brown, N, Jacob, DJ, Jaffe, DA, Kolb, CE, Lefohn, AS, Oltmans, S, Parrish, DD, Yarwood, G and **Zhang, L.** 2011. Establishing policy relevant background (PRB) ozone concentrations in the United States. *Environ Sci Technol* **45**(22): 9484–9497. DOI: https://doi.org/10.1021/es2022818

Mote, PW, Rupp, DE, Li, S, Sharp, DJ, Otto, F, Uhe, PF, Xiao, M, Lettenmaier, DP, Cullen, H and **Allen, MR.** 2016. Perspectives on the causes of exceptionally low 2015 snowpack in the western United States. *Geophys Res Lett* **43**: 10,980–10,988. DOI: https://doi.org/10.1002/2016GL069965

Müller, M, Anderson, BE, Beyersdorf, AJ, Crawford, JH, Diskin, GS, Eichler, P, Fried, A, Keutsch, FN, Mikoviny, T, Thornhill, KL, Walega, JG, Weinheimer, AJ, Yang, M, Yokelson, RJ and **Wisthaler, A.** 2016. In situ measurements and modeling of reactive trace gases in a small biomass burning plume. *Atmos Chem Phys* **16**(6): 3813–3824. DOI: https://doi.org/10.5194/acp-16-3813-2016

Musselman, RC and **Korfmacher, JL.** 2014. Ozone in remote areas of the Southern Rocky Mountains. *Atmos Environ* **82**: 383–390. DOI: https://doi.org/10.1016/j.atmosenv.2013.10.051

National Research Council (NRC). 2010. *Global sources of local pollution: An assessment of long-range transport of key air pollutants to and from the United States*. Board on Atmospheric Sciences and Climate, Committee on the Significance of International Transport of Air Pollutants. Washington, DC: The National Academies Press.

Neuman, JA, Trainer, M, Aikin, KC, Angevine, WM, Brioude, J, Brown, SS, de Gouw, JA, Dube, WP, Flynn, JH, Graus, M, Holloway, JS, Lefer, BL, Nedelec, P, Nowak, JB, Parrish, DD, Pollack, IB, Roberts, JM, Ryerson, TB, Smit, H, Thouret, V and **Wagner, NL.** 2012. Observations of ozone transport from the free troposphere to the Los Angeles basin. *J Geophys Res Atmos* **117**(D00): V09. DOI: https://doi.org/10.1029/2011jd016919

Newchurch, MJ, Ayoub, MA, Oltmans, S, Johnson, B and **Schmidlin, FJ.** 2003. Vertical distribution of ozone at four sites in the United States. *J Geophys Res Atmos* **108**(D1). DOI: https://doi.org/10.1029/2002jd002059

Orbe, C, Waugh, DW, Yang, H, Lamarque, JF, Tilmes, S and **Kinnison, DE.** 2017. Tropospheric transport differences between models using the same large-scale meteorological fields. *Geophys Res Lett* **44**(2): 1068–1078. DOI: https://doi.org/10.1002/2016gl071339

Ott, LE, Duncan, BN, Thompson, AM, Diskin, G, Fasnacht, Z, Langford, AO, Lin, MY, Molod, AM, Nielsen, JE, Pusede, SE, Wargan, K, Weinheimer, AJ and **Yoshida, Y.** 2016. Frequency and impact of summertime stratospheric intrusions over Maryland during DISCOVER-AQ (2011): New evidence from NASA's GEOS-5 simulations. *J Geophys Res Atmos* **121**(7): 3687–3706. DOI: https://doi.org/10.1002/2015jd024052

Parrish, DD, Aikin, KC, Oltmans, SJ, Johnson, BJ, Ives, M and **Sweeny, C.** 2010. Impact of transported background ozone inflow on summertime air quality in a California ozone exceedance area. *Atmos Chem Phys* **10**(20): 10093–10109. DOI: https://doi.org/10.5194/acp-10-10093-2010

Parrish, DD, Lamarque, JF, Naik, V, Horowitz, L, Shindell, DT, Staehelin, J, Derwent, R, Cooper, OR, Tanimoto, H, Volz-Thomas, A, Gilge, S, Scheel, HE, Steinbacher, M and **Frohlich, M.** 2014. Long-term changes in lower tropospheric baseline ozone concentrations: Comparing chemistry-climate models and observations at northern midlatitudes. *J Geophys Res Atmos* **119**(9): 5719–5736. DOI: https://doi.org/10.1002/2013jd021435

Parrish, DD, Law, KS, Staehelin, J, Derwent, R, Cooper, OR, Tanimoto, H, Volz-Thomas, A, Gilge, S, Scheel, HE, Steinbacher, M and **Chan, E.** 2012. Long-term changes in lower tropospheric baseline ozone concentrations at northern midlatitudes. *Atmos Chem Phys* **12**: 11485–11504. DOI: https://doi.org/10.5194/acp-12-11485-2012

Parrish, DD, Petropavlovskikh, I and **Oltmans, SJ.** 2017b. Reversal of long-term trend in baseline ozone concentrations at the North American West Coast. *Geophys Res Lett* **44**(20): 10,675–10,681. DOI: https://doi.org/10.1002/2017GL074960

Parrish, DD, Young, LM, Newman, MH, Aikin, KC and **Ryerson, TB.** 2017a. Ozone design values in Southern California's air basins: Temporal evolution and U.S. background contribution. *J Geophys Res Atmos* **122**(20): 11166–11182. DOI: https://doi.org/10.1002/2016jd026329

Pfister, GG, Walters, S, Emmons, LK, Edwards, DP and **Avise, J.** 2013. Quantifying the contribution of inflow on surface ozone over California during summer

2008. *J Geophys Res Atmos* **118**(21): 12282–12299. DOI: https://doi.org/10.1002/2013jd020336

Pierce, RB, Al-Saadi, JA, Schaack, T, Lenzen, A, Zapotocny, T, Johnson, D, Kittaka, C, Buker, M, Hitchman, MH, Tripoli, G, Fairlie, TD, Olson, JR, Natarajan, M, Crawford, J, Fishman, J, Avery, M, Browell, EV, Creilson, J, Kondo, Y and **Sandholm, ST.** 2003. Regional Air Quality Modeling System (RAQMS) predictions of the tropospheric ozone budget over east Asia. *J Geophys Res Atmos* **108**(D21). DOI: https://doi.org/10.1029/2002jd003176

Raffa, KF, Aukema, BH, Bentz, BJ, Carroll, AL, Hicke, JA, Turner, MG and **Romme, WH.** 2008. Cross-scale drivers of natural disturbances prone to anthropogenic amplification: The dynamics of bark beetle eruptions. *Bioscience* **58**(6): 501–517. DOI: https://doi.org/10.1641/b580607

Ramboll Environ. 2014. CAMx (Comprehensive Air Quality Model with Extensions) User's Guide Version 6.1. Novato, California: Ramboll Environ. Available at: http://www.camx.com/files/camxusersguide_v6–10.pdf.

Rastigejev, Y, Park, R, Brenner, MP and **Jacob, DJ.** 2010. Resolving intercontinental pollution plumes in global models of atmospheric transport. *J Geophys Res Atmos* **115**(D02): 302. DOI: https://doi.org/10.1029/2009jd012568

Reidmiller, DR, Fiore, AM, Jaffe, DA, Bergmann, D, Cuvelier, C, Dentener, FJ, Duncan, BN, Folberth, G, Gauss, M, Gong, S, Hess, P, Jonson, JE, Keating, T, Lupu, A, Marmer, E, Park, R, Schultz, MG, Shindell, DT, Szopa, S, Vivanco, MG, Wild, O and **Zuber, A.** 2009. The influence of foreign vs. North American emissions on surface ozone in the US. *Atmos Chem Phys* **9**(14): 5027–5042. DOI: https://doi.org/10.5194/acp-9-5027-2009

Russell, AR, Valin, LC and **Cohen, RC.** 2012. Trends in OMI NO_2 observations over the United States: Effects of emission control technology and the economic recession. *Atmos Chem Phys* **12**(24): 12197–12209. DOI: https://doi.org/10.5194/acp-12-12197-2012

Ryerson, TB, Andrews, AE, Angevine, WM, Bates, TS, Brock, CA, Cairns, B, Cohen, RC, Cooper, OR, de Gouw, JA, Fehsenfeld, FC, Ferrare, RA, Fischer, ML, Flagan, RC, Goldstein, AH, Hair, JW, Hardesty, RM, Hostetler, CA, Jimenez, JL, Langford, AO, McCauley, E, McKeen, SA, Molina, LT, Nenes, A, Oltmans, SJ, Parrish, DD, Pederson, JR, Pierce, RB, Prather, K, Quinn, PK, Seinfeld, JH, Senff, CJ, Sorooshian, A, Stutz, J, Surratt, JD, Trainer, M, Volkamer, R, Williams, EJ and **Wofsy, SC.** 2013. The 2010 California Research at the Nexus of Air Quality and Climate Change (CalNex) field study. *J Geophys Res Atmos* **118**(11): 5830–5866. DOI: https://doi.org/10.1002/jgrd.50331

Sandu, A, Daescu, DN, Carmichael, GR and **Chai, TF.** 2005. Adjoint sensitivity analysis of regional air quality models. *J Comput Phys* **204**(1): 222–252. DOI: https://doi.org/10.1016/j.jcp.2004.10.011

Schnell, JL, Prather, MJ, Josse, B, Naik, V, Horowitz, LW, Cameron-Smith, P, Bergmann, D, Zeng, G, Plummer, DA, Sudo, K, Nagashima, T, Shindell, DT, Faluvegi, G and **Strode, SA.** 2015. Use of North American and European air quality networks to evaluate global chemistry-climate modeling of surface ozone. *Atmos Chem Phys* **15**(18): 10581–10596. DOI: https://doi.org/10.5194/acp-15-10581-2015

Schultz, MG, Schroder, S, Lyapina, O, Cooper, OR, Galbally, I, Petropavlovskikh, I, von Schneidemesser, E, Tanimoto, H, Elshorbany, Y, Naja, M, Seguel, RJ, Dauert, U, Eckhardt, P, Feigenspan, S, Fiebig, M, Hjellbrekke, AG, Hong, YD, Kjeld, PC, Koide, H, Lear, G, Tarasick, D, Ueno, M, Wallasch, M, Baumgardner, D, Chuang, MT, Gillett, R, Lee, M, Molloy, S, Moolla, R, Wang, T, Sharps, K, Adame, JA, Ancellet, G, Apadula, F, Artaxo, P, Barlasina, ME, Bogucka, M, Bonasoni, P, Chang, L, Colomb, A, Cuevas-Agullo, E, Cupeiro, M, Degorska, A, Ding, AJ, FrHlich, M, Frolova, M, Gadhavi, H, Gheusi, F, Gilge, S, Gonzalez, MY, Gros, V, Hamad, SH, Helmig, D, Henriques, D, Hermansen, O, Holla, R, Hueber, J, Im, U, Jaffe, DA, Komala, N, Kubistin, D, Lam, KS, Laurila, T, Lee, H, Levy, I, Mazzoleni, C, Mazzoleni, LR, McClure-Begley, A, Mohamad, M, Murovec, M, Navarro-Comas, M, Nicodim, F, Parrish, D, Read, KA, Reid, N, Ries, NRL, Saxena, P, Schwab, JJ, Scorgie, Y, Senik, I, Simmonds, P, Sinha, V, Skorokhod, AI, Spain, G, Spangl, W, Spoor, R, Springston, SR, Steer, K, Steinbacher, M, Suharguniyawan, E, Torre, P, Trickl, T, Lin, WL, Weller, R, Xu, XB, Xue, LK and **Ma, ZQ.** 2017. Tropospheric Ozone Assessment Report: Database and Metrics Data of Global Surface Ozone Observations. *Elementa* **5**(58). DOI: https://doi.org/10.1525/elementa.244

Shen, L and **Mickley, LJ.** 2017. Seasonal prediction of US summertime ozone using statistical analysis of large scale climate patterns. *PNAS* **114**: 2491–2496. DOI: https://doi.org/10.1073/pnas.1610708114

Sherwen, T, Evans, MJ, Carpenter, LJ, Schmidt, JA and **Mickely, LJ.** 2017. Halogen chemistry reduces tropospheric O_3 radiative forcing. *Atmos Chem Phys* **17**: 1557–1569. DOI: https://doi.org/10.5194/acp-17-1557-2017

Silva, RA, West, JJ, Zhang, Y, Anenberg, SC, Lamarque, J-F, Shindell, DT, Collins, WJ, Dalsoren, S, Faluvegi, G, Folberth, G, Horowitz, LW, Nagashima, T, Naik, V, Rumbold, S, Skeie, R, Sudo, K, Takemura, T, Bergmann, D, Cameron-Smith, P, Cionni, I, Doherty, RM, Eyring, V, Josse, B, MacKenzie, IA, Plummer, D, Righi, M, Stevenson, DS, Strode, S, Szopa, S and **Zeng, G.** 2013. Global premature mortality due to anthropogenic outdoor air pollution and the contribution of past climate change. *Environ Res Lett* **8**(3). DOI: https://doi.org/10.1088/1748-9326/8/3/034005

Simon, H, Baker, KR and **Phillips, S.** 2012. Compilation and interpretation of photochemical model performance statistics published between 2006 and

2012. *Atmos Environ* **61**: 124–139. DOI: https://doi.org/10.1016/j.atmosenv.2012.07.012

Simon, H, Reff, A, Wells, B, Xing, J and **Frank, N.** 2015. Ozone trends across the United States over a period of decreasing NO_x and VOC emissions. *Environ Sci Technol* **49**(1): 186–195. DOI: https://doi.org/10.1021/es504514z

Singh, HB, Cai, C, Kaduwela, A, Weinheimer, A and **Wisthaler, A.** 2012. Interactions of fire emissions and urban pollution over California: Ozone formation and air quality simulations. *Atmos Environ* **56**: 45–51. DOI: https://doi.org/10.1016/j.atmosenv.2012.03.046

Skerlak, B, Sprenger, M and **Wernli, H.** 2014. A global climatology of stratosphere-troposphere exchange using the ERA-Interim data set from 1979 to 2011. *Atmos Chem Phys* **14**(2): 913–937. DOI: https://doi.org/10.5194/acp-14-913-2014

Stauffer, RM, Thompson, AM, Oltmans, SJ and **Johnson, BJ.** 2017. Tropospheric ozonesonde profiles at long-term US monitoring sites: 2. Links between Trinidad Head, CA, profile clusters and inland surface ozone measurements. *J Geophys Res Atmos* **122**(2): 1261–1280. DOI: https://doi.org/10.1002/2016jd025254

Stock, ZS, Russo, MR, Butler, TM, Archibald, AT, Lawrence, MG, Telford, PJ, Abraham, NL and **Pyle, JA.** 2013. Modelling the impact of megacities on local, regional and global tropospheric ozone and the deposition of nitrogen species. *Atmos Chem Phys* **13**(24): 12215–12231. DOI: https://doi.org/10.5194/acp-13-12215-2013

Strode, SA, Rodriguez, JM, Logan, JA, Cooper, OR, Witte, JC, Lamsal, LN, Damon, M, Aartsen, BV, Steenrod, SD and **Strahan, SE.** 2015. Trends and variability in surface ozone over the United States. *J Geophys Res Atmos* **120**(17): 9020–9042. DOI: https://doi.org/10.1002/2014JD022784

Sullivan, JT, McGee, TJ, Thompson, AM, Pierce, RB, Sumnicht, GK, Twigg, L, Eloranta, E and **Hoff, RM.** 2015. Characterizing the lifetime and occurrence of stratospheric-tropospheric exchange events in the rocky mountain region using high-resolution ozone measurements. *J Geophys Res Atmos* **120**(24): 12410–12424. DOI: https://doi.org/10.1002/2015jd023877

Teakles, AD, So, R, Ainslie, B, Nissen, R, Schiller, C, Vingarzan, R, McKendry, I, Macdonald, AM, Jaffe, DA, Bertram, AK, Strawbridge, KB, Leaitch, WR, Hanna, S, Toom, D, Baik, J and **Huang, L.** 2017. Impacts of the July 2012 Siberian fire plume on air quality in the Pacific Northwest. *Atmos Chem Phys* **17**(4): 2593–2611. DOI: https://doi.org/10.5194/acp-17-2593-2017

Travis, KR, Jacob, DJ, Fisher, JA, Kim, PS, Marais, EA, Zhu, L, Yu, K, Miller, CC, Yantosca, RM, Sulprizio, MP, Thompson, AM, Wennberg, PO, Crounse, JD, St Clair, JM, Cohen, RC, Laughner, JL, Dibb, JE, Hall, SR, Ullmann, K, Wolfe, GM, Pollack, IB, Peischl, J, Neuman, JA and **Zhou, XL.** 2016. Why do models overestimate surface ozone in the Southeast United States? *Atmos Chem Phys* **16**(21): 13561–13577. DOI: https://doi.org/10.5194/acp-16-13561-2016

Travis, KR, Jacob, DJ, Keller, CA, Kuang, S, Lin, J, Newchurch, MJ and **Thompson, AM.** 2017. Resolving ozone vertical gradients in air quality models. *Atmos Chem Phys Discuss* **2017**: 1–18. DOI: https://doi.org/10.5194/acp-2017-596

U.S. Environmental Protection Agency (US EPA). 2013. Integrated Science Assessment (ISA) of Ozone and Related Photochemical Oxidants (Final Report, Feb 2013). Washington, DC: U.S. Environmental Protection Agency. EPA/600/R-10/076F. Available at: https://cfpub.epa.gov/ncea/isa/recordisplay.cfm?deid=247492 Accessed October 27, 2017.

U.S. Environmental Protection Agency (US EPA). 2014a. Meteorological Model Performance for Annual 2011 WRF v3.4 Simulation. Office of Air Quality Planning and Standards. Available at: https://www3.epa.gov/ttn/scram/reports/MET_TSD_2011_final_11-26-14.pdf Accessed October 27, 2017.

U.S. Environmental Protection Agency (US EPA). 2014b. Technical Support Documentation, EPA Region 8 Review of a Flagging Demonstration by the Wyoming Department of Environmental Quality, Division of Air Quality, Ozone NAAQS Exceedances Occurring June 14, 2012, Big Piney and Boulder Monitoring Station. Available at: https://www.epa.gov/sites/production/files/2015-05/documents/tsd_strat_o3_june_14_2012_wyo.pdf Accessed October 27, 2017.

U.S. Environmental Protection Agency (US EPA). 2014c. Policy Assessment for the Review of the Ozone National Ambient Air Quality Standards, Final Report. Research Triangle Park, NC: U.S. Environmental Protection Agency, Office of Air and Radiation, Office of Air Quality Planning and Standards. EPA-452/R-14-006. August 2014. Available at: https://www3.epa.gov/ttn/naaqs/standards/ozone/data/20140829pa.pdf Accessed January 4, 2018.

U.S. Environmental Protection Agency (US EPA). 2015. Implementation of the 2015 Primary Ozone NAAQS: Issues Associated with Background Ozone, White Paper for Discussion. Washington, DC: U.S. Environmental Protection Agency. Available at: https://www.epa.gov/sites/production/files/2016–03/documents/whitepaper-bgo3-final.pdf Accessed October 27, 2017.

U.S. Environmental Protection Agency (US EPA). 2016a. Treatment of Data Influenced by Exceptional Events. 81 FR, 68216, October 3, 2016. Available at: https://www.epa.gov/sites/production/files/2016-09/documents/exceptional_events_rule_revisions_2060-as02_final.pdf Accessed October 27, 2017.

U.S. Environmental Protection Agency (US EPA). 2016b. Guidance on the Preparation of Exceptional Events Demonstrations for Wildfire Events that May Influence Ozone Concentrations. Research Triangle Park, NC: U.S. Environmental Protection Agency, Office of Air Quality Planning and Standards. Available at: https://www.epa.

gov/sites/production/files/2016-09/documents/exceptional_events_guidance_9-16-16_final.pdf Accessed October 27, 2017.

U.S. Environmental Protection Agency (US EPA). 2016c. Air Quality Modeling Technical Support Document for the 2015 Ozone NAAQS Preliminary Interstate Transport Assessment. Research Triangle Park, NC: U.S. Environmental Protection Agency, Office of Air Quality Planning and Standards. Available at: https://www.epa.gov/sites/production/files/2017-01/documents/aq_modeling_tsd_2015_o3_naaqs_preliminary_interstate_transport_assessmen.pdf Accessed October 27, 2017.

U.S. Global Change Research Program (US GCRP). 2016. The Impacts of Climate Change on Human Health in the United States: A Scientific Assessment. Crimmins, A, Balbus, J, Gamble, JL, Beard, CB, Bell, JE, et al. (eds.). Washington, D.C.: U.S. Global Change Research Program. Accessed January 22, 2018. DOI: https://.doi.org/10.7930/J0R49NQX

Val Martin, M, Heald, CL and **Arnold, SR.** 2014. Coupling dry deposition to vegetation phenology in the Community Earth System Model: Implications for the simulation of surface O_3. *Geophys Res Lett* **41**(8): 2988–2996. DOI: https://doi.org/10.1002/2014GL059651

Verstraeten, WW, Neu, JL, Williams, JE, Bowman, KW, Worden, JR and **Boersma, KF.** 2015. Rapid increases in tropospheric ozone production and export from China. *Nat Geosci* **8**(9): 690–695. DOI: https://doi.org/10.1038/ngeo2493

Wang, HQ, Jacob, DJ, Le Sager, P, Streets, DG, Park, RJ, Gilliland, AB and **van Donkelaar, A.** 2009. Surface ozone background in the United States: Canadian and Mexican pollution influences. *Atmos Environ* **43**: 1310–1319. DOI: https://doi.org/10.1016/j.atmosenv.2008.11.036

Wang, YH, Jacob, DJ and **Logan, JA.** 1998. Global simulation of tropospheric O_3-NO_x-hydrocarbon chemistry: 3. Origin of tropospheric ozone and effects of nonmethane hydrocarbons. *J Geophys Res Atmos* **103**(D9): 10757–10767. DOI: https://doi.org/10.1029/98jd00156

Weaver, CP, Liang, XZ, Zhu, J, Adams, PJ, Amar, P, Avise, J, Caughey, M, Chen, J, Cohen, RC, Cooter, E, Dawson, JP, Gilliam, R, Gilliland, A, Goldstein, AH, Grambsch, A, Grano, D, Guenther, A, Gustafson, WI, Harley, RA, He, S, Hemming, B, Hogrefe, C, Huang, HC, Hunt, SW, Jacob, DJ, Kinney, PL, Kunkel, K, Lamarque, JF, Lamb, B, Larkin, NK, Leung, LR, Liao, KJ, Lin, JT, Lynn, BH, Manomaiphiboon, K, Mass, C, McKenzie, D, Mickley, LJ, O'Neill, SM, Nolte, C, Pandis, SN, Racherla, PN, Rosenzweig, C, Russell, AG, Salathe, E, Steiner, AL, Tagaris, E, Tao, Z, Tonse, S, Wiedinmyer, C, Williams, A, Winner, DA, Woo, JH, Wu, S and **Wuebbles, DJ.** 2009. A preliminary synthesis of modeled climate change impacts on US regional ozone concentrations. *Bull Am Meteorol Soc* **90**(12): 1843–1863. DOI: https://doi.org/10.1175/2009bams2568.1

Weiss-Penzias, P, Jaffe, DA, Swartzendruber, P, Dennison, JB, Chand, D, Hafner, W and **Prestbo, E.** 2006. Observations of Asian air pollution in the free troposphere at Mount Bachelor Observatory during the spring of 2004. *J Geophys Res* **111**(D10). DOI: https://doi.org/10.1029/2005JD006522

Western Air Quality Study (WAQS). 2017. Western Air Quality 2011b Modeling Platform. Available at: http://vibe.cira.colostate.edu/wiki/wiki/%209166/waqs-2011b-modeling-platform Accessed November 7, 2017.

Wigder, NL, Jaffe, DA, Herron-Thorpe, FL and **Vaughan, JK.** 2013a. Influence of daily variations in baseline ozone on urban air quality in the United States Pacific Northwest. *J Geophys Res Atmos* **118**(8): 3343–3354. DOI: https://doi.org/10.1029/2012JD018738

Wigder, NL, Jaffe, DA and **Saketa, FA.** 2013b. Ozone and particulate matter enhancements from regional wildfires observed at Mount Bachelor during 2004–2011. *Atmos Environ* **75**: 24–31. DOI: https://doi.org/10.1016/j.atmosenv.2013.04.026

Wild, O, Fiore, AM, Shindell, DT, Doherty, RM, Collins, WJ, Dentener, FJ, Schultz, MG, Gong, S, MacKenzie, IA, Zeng, G, Hess, P, Duncan, BN, Bergmann, DJ, Szopa, S, Jonson, JE, Keating, TJ and **Zuber, A.** 2012. Modelling future changes in surface ozone: A parameterized approach. *Atmos Chem Phys* **12**(4): 2037–2054. DOI: https://doi.org/10.5194/acp-12-2037-2012

Witman, S, Holloway, T and **Reddy, PJ.** 2014. Integrating satellite data into air quality management: Experience from Colorado. *EM*, 34–38. February 2014.

Wu, SL, Duncan, BN, Jacob, DJ, Fiore, AM and **Wild, O.** 2009. Chemical nonlinearities in relating intercontinental ozone pollution to anthropogenic emissions. *Geophys Res Lett* **36**(L05): 806. DOI: https://doi.org/10.1029/2008GL036607

Wyoming Department of Environmental Quality (WYDEQ). 2012. Exceptional Event Demonstration Package for the Environmental Protection Agency: Big Piney and Boulder, Wyoming Ozone Standard Exceedances June 14, 2012. Cheyenne, WY: State of Wyoming Department of Environmental Quality/Air Quality Division. Available at: https://www.epa.gov/air-quality-analysis/exceptional-events-documents-ozone-wyoming Accessed October 27, 2017.

Xing, J, Mathur, R, Pleim, J, Hogrefe, C, Gan, CM, Wong, DC, Wei, C, Gilliam, R and **Pouliot, G.** 2015. Observations and modeling of air quality trends over 1990–2010 across the Northern Hemisphere: China, the United States and Europe. *Atmos Chem Phys* **15**(5): 2723–2747. DOI: https://doi.org/10.5194/acp-15-2723-2015

Xing, J, Mathur, R, Pleim, J, Hogrefe, C, Wang, JD, Gan, CM, Sarwar, G, Wong, DC and **McKeen, S.** 2016. Representing the effects of stratosphere-troposphere exchange on 3-D O-3 distributions in chemistry transport models using a potential vorticity-based parameterization. *Atmos Chem Phys* **16**(17): 10865–10877. DOI: https://doi.org/10.5194/acp-16-10865-2016

Xu, L, Yu, JY, Schnell, JL and **Prather, MJ.** 2017. The seasonality and geographic dependence of ENSO impacts on US surface ozone variability. *Geophys Res Lett* **44**(7): 3420–3428. DOI: https://doi.org/10.1002/2017gl073044

Yates, EL, Iraci, LT, Roby, MC, Pierce, RB, Johnson, MS, Reddy, PJ, Tadic, JM, Loewenstein, M and **Gore, W.** 2013. Airborne observations and modeling of springtime stratosphere-to-troposphere transport over California. *Atmos Chem Phys* **13**(24): 12481–12494. DOI: https://doi.org/10.5194/acp-13-12481-2013

Ying, Q and **Krishnan, A.** 2010. Source contributions of volatile organic compounds to ozone formation in southeast Texas. *J Geophys Res Atmos* **115**(D17): 306. DOI: https://doi.org/10.1029/2010jd013931

Zhang, L, Jacob, DJ, Boersma, KF, Jaffe, DA, Olson, JR, Bowman, KW, Worden, JR, Thompson, AM, Avery, MA, Cohen, RC, Dibb, JE, Flock, FM, Fuelberg, HE, Huey, LG, McMillan, WW, Singh, HB and **Weinheimer, AJ.** 2008. Transpacific transport of ozone pollution and the effect of recent Asian emission increases on air quality in North America: An integrated analysis using satellite, aircraft, ozonesonde, and surface observations. *Atmos Chem Phys* **8**: 6117–6136. DOI: https://doi.org/10.5194/acp-8-6117-2008

Zhang, L, Jacob, DJ, Downey, NV, Wood, DA, Blewitt, D, Carouge, CC, van Donkelaar, A, Jones, DBA, Murray, LT and **Wang, Y.** 2011. Improved estimate of the policy-relevant background ozone in the United States using the GEOS-Chem global model with 1/2 degrees × 2/3 degrees horizontal resolution over North America. *Atmos Environ* **45**(37): 6769–6776. DOI: https://doi.org/10.1016/j.atmosenv.2011.07.054

Zhang, L, Jacob, DJ, Kopacz, M, Henze, DK, Singh, K and **Jaffe, DA.** 2009. Intercontinental source attribution of ozone pollution at western US sites using an adjoint method. *Geophys Res Lett* **36**(L11): 810. DOI: https://doi.org/10.1029/2009GL037950

Zhang, L, Jacob, DJ, Yue, X, Downey, NV, Wood, DA and **Blewitt, D.** 2014. Sources contributing to background surface ozone in the US Intermountain West. *Atmos Chem Phys* **14**(11): 5295–5309. DOI: https://doi.org/10.5194/acp-14-5295-2014

Zhang, L and **Jaffe, DA.** 2017. Trends and sources of ozone and sub-micron aerosols at the Mt. Bachelor Observatory (MBO) during 2004–2015. *Atmos Environ* **165**: 143–154. DOI: https://doi.org/10.1016/j.atmosenv.2017.06.042

Zhou, W, Cohan, DS and **Napelenok, SL.** 2013. Reconciling NO_x emissions reductions and ozone trends in the US, 2002–2006. *Atmos Environ* **70**: 236–244. DOI: https://doi.org/10.1016/j.atmosenv.2012.12.038

Ziemke, JR, Chandra, S, Labow, GJ, Bhartia, PK, Froidevaux, L and **Witte, JC.** 2011. A global climatology of tropospheric and stratospheric ozone derived from Aura OMI and MLS measurements. *Atmos Chem Phys* **11**(17): 9237–9251. DOI: https://doi.org/10.5194/acp-11-9237-2011

Zoogman, P, Jacob, DJ, Chance, K, Liu, X, Lin, M, Fiore, A and **Travis, K.** 2014. Monitoring high-ozone events in the US Intermountain West using TEMPO geostationary satellite observations. *Atmos Chem Phys* **14**(12): 6261–6271. DOI: https://doi.org/10.5194/acp-14-6261-2014

Zoogman, P, Liu, X, Suleiman, RM, Pennington, WF, Flittner, DE, Al-Saadi, JA, Hilton, BB, Nicks, DK, Newchurch, MJ, Carr, JL, Janz, SJ, Andraschko, MR, Arola, A, Baker, BD, Canova, BP, Chan Miller, C, Cohen, RC, Davis, JE, Dussault, ME, Edwards, DP, Fishman, J, Ghulam, A, González Abad, G, Grutter, M, Herman, JR, Houck, J, Jacob, DJ, Joiner, J, Kerridge, BJ, Kim, J, Krotkov, NA, Lamsal, L, Li, C, Lindfors, A, Martin, RV, McElroy, CT, McLinden, C, Natraj, V, Neil, DO, Nowlan, CR, O'Sullivan, EJ, Palmer, PI, Pierce, RB, Pippin, MR, Saiz-Lopez, A, Spurr, RJD, Szykman, JJ, Torres, O, Veefkind, JP, Veihelmann, B, Wang, H, Wang, J and **Chance, K.** 2017. Tropospheric emissions: Monitoring of pollution (TEMPO). *J Quant Spectrosc Radiat Transfer* **186**(Supplement C): 17–39. DOI: https://doi.org/10.1016/j.jqsrt.2016.05.008

How to cite this article: Jaffe, DA, Cooper, OR, Fiore, AM, Henderson, BH, Tonnesen, GS, Russell, AG, Henze, DK, Langford, AO, Lin, M and Moore, T. 2018. Scientific assessment of background ozone over the U.S.: Implications for air quality management. *Elem Sci Anth*, 6: 56. DOI: https://doi.org/10.1525/elementa.309

Domain Editor-in-Chief: Detlev Helmig, Ph.D., Institute of Alpine and Arctic Research, University of Colorado Boulder, US

Associate Editor: Allen Goldstein, University of California Berkeley, US

Knowledge Domain: Atmospheric Science

Submitted: 06 February 2018 **Accepted:** 24 June 2018 **Published:** 30 July 2018